Zeitschrift: Schweizerische mineralogische und petrographische Mitteilungen = Bulletin suisse de minéralogie et pétrographie

Band: 85 (2005)

Heft: 2-3: Central Alps

Artikel: Eclogite relics in the Central Alps : PT-evolution, Lu-Hf ages and implications for formation of tectonic mélange zones

Autor: Brouwer, F.M. / Burri, T. / Engi, M.

DOI: https://doi.org/10.5169/seals-1658

Schweizerische Mineralogische und Petrographische Mitteilungen 85, 147–174, 2005

Eclogite relics in the Central Alps: PT - evolution, Lu–Hf ages and implications for formation of tectonic mélange zones

F.M. Brouwer[1,2], *T. Burri*[1,3], *M. Engi*[1] and *A. Berger*[1]

Abstract

Mafic rocks containing eclogite relics are fairly widespread in the crystalline nappe stack of the Swiss Central Alps. This study addresses the spatial distribution of eclogite relics in the Central Alps, their field relations, structural and petrological characteristics, and their PTt-history. Implications for the assembly of the nappe stack are explored.

The majority of eclogite-facies relics is confined to a single super-unit of tectonic mélange, interpreted as a tectonic accretion channel (TAC). Numerous mafic high-pressure (HP) lenses have been discovered through systematic fieldwork in the TAC units of the Central Alps, an up-to-date inventory of which is presented. Systematic documentation of select samples with HP imprint yields clockwise PT-paths. Prograde phase relations are seldom preserved, except in the chemical zoning of garnet porphyroblasts. However, when present, relic assemblages indicate HP-LT conditions indicative of a subduction setting. Maximum recorded pressures are substantially different from one location to the next (1.9 to 3.3 GPa). Depending on the degree of rehydration, reaction sequences are derived from observed relics, local replacement relations and assemblages. Quantitative constraints on the detailed PT-path are extracted by combining isochemical phase diagrams and *TWQ*-thermobarometry with petrographic information. HP lenses from different locations display substantially different paths, both within and between different mélange zones of the TAC. PT-conditions reflecting the late-Alpine Barrovian overprint of mafic HP lenses are in agreement with the coherent regional pattern derived from metasediments, i.e., maximum temperatures (~600 °C in the central Lepontine belt, 700–750 °C in the southern parts) were reached at pressures between 0.75 and 0.55 GPa

Four samples have been dated by Lu–Hf isotopic analysis of garnet, clinopyroxene, matrix phases and whole-rock powders. The age span covers a range from >70 to ~36 Ma, much larger than previously documented for Alpine HP rocks from the Central Alps. Petrological data of the samples and their Lu–Hf isotopic system indicate a protracted HP history for at least some of the sub-units of the TAC, with garnet growth under eclogite-facies conditions starting before 70 Ma in some parts of the TAC, and continuing as late as 36 Ma in others.

These data have implications for the dynamics of mélange formation within the TAC, with internal fragmentation and mixing, and pronounced mobility of the tectonic zones, probably during the early, subductional stages and again during the post-collisional extrusion along the plate boundary. After 32 Ma, when the Barrovian overprint reached its maximum temperature, the TAC appears to have been exhumed as part of the then-coherent crystalline nappe stack.

Keywords: eclogite, garnet amphibolite, Central Alps, Southern Steep Belt, Lu–Hf geochronology, PT-evolution, Tectonic Accretion Channel.

Introduction

In collisional orogens, former plate boundaries are often represented by mélange-like lithological associations that formed in the subduction zone that previously marked the plate margin (e.g. Liu et al., 2004; Federico et al., 2005; Stöckhert and Gerya, 2005). These mélanges are generally a composite of ortho- and paragneisses, with less common fragments of marble, calc-silicate, mafic and ultramafic rocks. In the Central Alps, the lithosphere-scale mélange (Trommsdorff, 1990) has been termed Tectonic Accretion Channel (TAC, Engi et al., 2001a) and it contains the vast majority of relics of high-pressure (HP) metamorphism present in the Central Alps. More recently, similar lithosphere-scale mélange zones in the Western Alps and the Himalayan Tso Morari region have been labelled 'tectonic shuffle zones' (Forster et al., 2006). The TAC is similar to type D

[1] Institut für Geologie, Universität Bern, Baltzerstrasse 1-3, CH-3012 Bern, Switzerland. <engi@geo.unibe.ch> <berger@geo.unibe.ch>
[2] Present address: Dept. of Petrology - FALW, Vrije Universiteit, De Boelelaan 1085, NL-1081 HV Amsterdam, The Netherlands. <fraukje.brouwer@falw.vu.nl>
[3] Present address: Kellerhans+Haefeli AG, Kapellenstrasse 22, CH-3011 Bern, Switzerland. <tombur@bluewin.ch>

0036-7699/05/0085/147

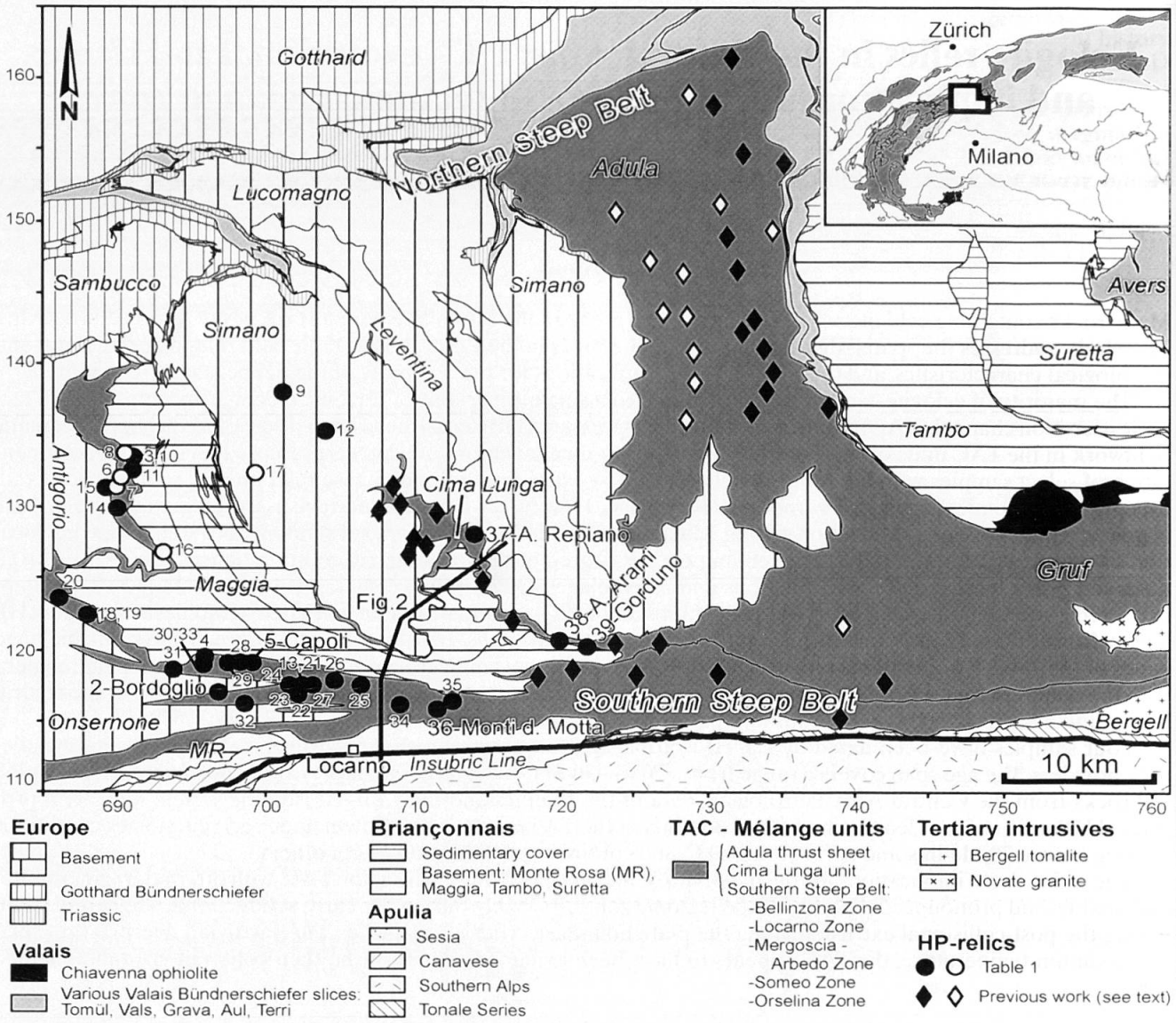

Fig. 1 Tectonic map of the Central Alps based on Berger and Mercolli (2006). Inset in the top right provides an overview of the Alpine mountain chain, with the location of the enlarged map indicated with a box. TAC mélange units are marked in dark grey. Locations of HP relics are indicated with circles (petrography summarised in Table 1) and diamonds (Adula-Cima Lunga system, compiled from the literature, see text for references). Filled symbols denote unambiguous evidence of HP metamorphism, open symbols indicate that textural evidence suggests HP, but is ambiguous. Location 1 (Porcaresc) is just off the map, about 5 km due west of location 18/19. Black line west of the lower centre indicates the cross section of Fig. 2.

and E subduction channels (Cloos and Shreve, 1988), but differs in that the accretion process also affects slices of the basement of the subducting plate and not just the sediments. Although exceptions exist, HP mineral assemblages are preserved as relics mostly in less deformed mafic and ultramafic rocks, and these assemblages predate the Barrovian metamorphic overprint commonly associated with final exhumation. This study aims to provide a comprehensive overview of the HP relics in the Central Alps, and insight in the processes that operated in the TAC. These processes resulted in differential movements of fragments that are recorded as variations in their PTt-paths. The paths are constrained by integrating geochronological data with petrological information, in the context of the tectonic setting and the distribution of HP relics within it.

The preferential preservation of HP relics in mafic rocks probably reflects the fact that their HP mineral assemblage is almost entirely composed of anhydrous phases: garnet, clinopyrox-

ene, quartz, kyanite, olivine, orthopyroxene, and rutile. Pargasitic hornblende is a common minor phase attributed to the eclogite facies (Heinrich, 1982). Retrograde reactions in mafic and ultramafic rocks were triggered by infiltration of significant amounts of a hydrous fluid. As a consequence, HP relics are often found to be armoured by a mantle of amphibolite-facies rocks of similar composition but higher water content (e.g. Heinrich, 1982; Heinrich, 1986; Terry et al., 2000). In addition, the relics frequently display various types and degrees of retrogression, due to restricted fluid influx.

Whereas discovering and recognising such relics in the field is a problem, interpreting their history correctly from observed textures, phase assemblages and mineral compositions is more demanding. Thermodynamic computation is an elegant approach to investigate the significance of the observed phase relations and interpret reaction textures. In this study we investigate in detail the history of partially retrogressed mafic HP rocks from the Central Alps of Switzerland. Based on a set of criteria to identify relics of HP metamorphism, an extended inventory of Alpine HP rocks in the Central Alps is presented. Phase diagrams are computed to investigate observed phase relations and reaction textures and to discuss their significance in terms of the recorded PT-evolution. Four samples were dated by Lu–Hf geochronology and the combined results of the techniques are used to discuss Alpine geodynamics, and specifically the processes operative during formation and exhumation of the TAC units.

Geology of the study area

The European Central Alps are the result of at least two cycles of ocean subduction and continent collision (Schmid et al., 2004): After southward subduction of the Piedmont-Ligurian Ocean below the Apulian plate during the late Cretaceous and early Paleogene, collision between Apulia and the Briançonnais terrane occurred during the early Eocene. HP rocks in the Monte-Rosa nappe, for example, result from this phase of continental subduction (e.g. Engi et al., 2001b). Garnet-clinopyroxene Sm–Nd (Becker, 1993) and zircon U–Pb SHRIMP dating (Gebauer, 1996) of eclogites from Alpe Arami (Fig. 1) yielded interpreted HP ages of 37.5 ± 2.2 and 35.8 ± 2.8 Ma, respectively. After collision, the oceanic lithosphere of the narrow Valais basin was subducted underneath the northern margin of the Briançonnais and was followed by the southernmost margin of the European continent. Continental collision then led to the formation of the nappe stack of the Central Alps and eventually to southward directed back-thrusting of the Alpine nappe pile along the Periadriatic Lineament between ~28–18 Ma (e.g. Schmid et al., 1996). Finally, decreased erosional efficiency in the crystalline core of the orogen caused a transition from dominantly vertical to horizontal extrusion, which in turn led to northward displacement of the deformation front when the Jura Mountains started to form some 14 Ma ago (Schlunegger and Simpson, 2002).

The Lepontine area is the metamorphic core of the Central Alps, and its current isograd pattern is attributed to the late Barrovian overprint that resulted from the emplacement of hot tectonic units at relatively shallow crustal levels (28–20 Ma, Engi et al., 1995). The highest, upper amphibolite-facies conditions were recorded between Locarno and the Bergell intrusive body along the Insubric Line (e.g. Engi et al., 1995). Exhumation of this high-grade metamorphic area resulted from back-thrusting of the nappe stack along the Periadriatic Lineament and from movement along overlying normal faults (e.g. Simplon fault, Mancktelow, 1991). The Lepontine dominantly consists of continental basement nappes separated by shear zones (Timar-Geng et al., 2004) and highly attenuated, locally discontinuous post-Variscan sedimentary rocks (e.g. Wenk, 1953). Slices of mafic and ultramafic rock (<1 km length), derived from oceanic crust, are locally wedged between the slices of continental origin. Due to polyphase deformation and metamorphism, attribution of tectonic slices to paleotectonic units is delicate. Recent studies, however, assign the different nappes and fragments to three domains (Fig. 1, Schmid, et al., 2004; Berger et al., 2005). The Gotthard, Antigorio, Leventina and Simano units are thought to have been derived from the southernmost European margin. The overlying Cima Lunga and Adula units, are made up of slices of continental origin, but also contain oceanic rocks, which often show unambiguous evidence of HP metamorphism. Units from the Southern Steep Belt (mainly the Mergoscia-Arbedo and Orselina zones, Engi, et al., 2001a; Burri, 2005), as well as the Someo zone (Pfeifer et al., 1991), share these characteristics. All these units have been assigned to a TAC that represents an exhumed subduction channel (Engi et al., 2001a). Individual slices in the mélange may derive from the Briançonnais fragment, the Valais oceanic domain or the European margin. The units overlying the TAC units (Monte Rosa, Maggia, Tambo, Suretta) are interpreted as parts of the Briançonnais continental fragment. Paleogeographic units derived

from south of the Briançonnais can not be unambiguously identified in the Lepontine, but do occur to its east and west.

The central part of the Lepontine area is defined by roughly flat-lying structures, whereas structural steep belts define the northern and southern limits. The Southern Steep Belt (SSB) is defined by vertical to overturned structures (Fig. 2). The formation of the SSB is related to a phase of backfolding and backthrusting, largely responsible for the exhumation of the Lepontine dome (e.g. Schmid et al., 1989). In the south, the SSB grades into the migmatites and mylonites of the Insubric Line, the Lepontine section of the Periadriatic Lineament marking the suture between the Briançonnais and Apulian continental segments. At the Insubric Line, high-grade Lepontine units are juxtaposed with the Southern Alps, which, during the Tertiary, have only experienced low-grade metamorphism.

The metamorphic grade in the Lepontine area varies from greenschist facies in the north to upper amphibolite facies in the south (Todd and Engi, 1997, and references therein). Although amphibolite-facies metamorphism is dominant in the central and southern Lepontine, relics of HP and sparse granulite-facies metamorphism are found as well (see reviews in Frey et al., 1999). HP relics are limited to a few distinct units: Adula, Cima Lunga, and the SSB (Figs. 1,2). Although HP relics are relatively common in these units, the majority of rocks displays amphibolite-facies assemblages, attributed to a Barrovian overprint of the Central Alps. It is unclear whether the dominance of amphibolite-facies rocks is merely a result of the strong Barrovian overprint, or if only a minority of rocks have in fact experienced HP metamorphism.

The HP units of the Central Alps are interpreted as a lithospheric mélange (Trommsdorff, 1990) or TAC (Engi, et al., 2001a), based on the fragmented and lithologically variable characteristics of these units. Slices of continental and oceanic crust may delaminate from subducting units and become part of the subduction channel, which may also incorporate mantle fragments. This process leads to the formation of heterogeneous units with a very fragmentary character. The size of individual slices is on the order of decimetres to kilometres. Internal deformation of the TAC and differential back-flow of fragments is likely to result in different PT-paths, each characteristic for the pertinent fragment (Engi et al., 2001a).

Regional distribution of HP rocks

Many occurrences of HP rocks in the Central Alps are well known and thoroughly investigated (e.g. Wang, 1939; Forster, 1947; Heinrich, 1986; Pfeifer, et al., 1991; Frey and Ferreiro Mählmann, 1999; Engi, et al., 2001a). Relatively coherent HP units (TAC) from the Central Alps are the Orselina zone in the SSB and the Adula and Cima Lunga mélange units, which have comparable tectonic positions and lithologic contents (Fig. 1). Although internally fragmented and composed of a variety of rock types, these units form distinct zones, which can be distinguished from the surrounding coherent nappes. Additional evidence of HP metamorphism is found in the Someo and Mergoscia-Arbedo zones of the SSB (locations marked in Bächlin et al., 1974; Spicher, 1980; Berger and Mercolli, 2006), which has not been systematically investigated with modern methods

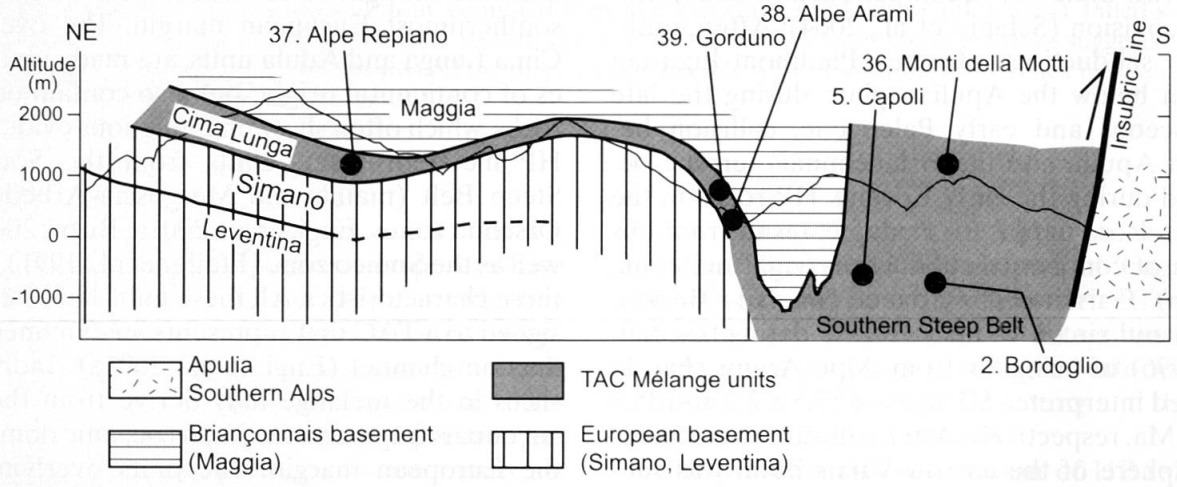

Fig. 2 Schematic cross section in the area between Val Verzasca and Valle Leventina (after Burri, 2005). Most samples discussed in this contribution are projected into this section (Fig. 1, Table 1). Line of section is indicated in Fig. 1; no vertical exaggeration.

(see however Grandjean, 2001). Between Locarno and Domodossola (just west of the study area), evidence of HP metamorphism is sparse but has been described by several authors (Kobe, 1956; Colombi and Pfeifer, 1986; Pfeifer et al., 1991). More widespread evidence of HP is again found west of Valle d'Ossola, in the Saas-Zermatt and Antrona units; the latter has been interpreted as equivalent to the ophiolite-bearing Orselina zone in the SSB (Colombi and Pfeifer, 1986).

Recent HP research, except for a few contributions (Colombi and Pfeifer, 1986; Pfeifer et al., 1991; Brouwer, 2000; Tóth et al., 2000; Grandjean, 2001), has mostly concentrated on the Adula and Cima Lunga units and on the famous Alpe Arami outcrops (e.g. Heinrich, 1986; Pfiffner and Trommsdorff, 1998; Dobrzhinetskaya et al., 2002; Dale and Holland, 2003; Bocchio et al., 2004, and many others). As a result of our current investigation, an updated inventory of relics of HP metamorphism in the Central Alps, and discussion of its implications have become possible. Especially west and northwest of Locarno several new occurrences of retrogressed eclogites were identified. In figures 1 we have compiled all of the published and new occurrences of HP rocks in the area between Valle Mesolcina and Valle d'Ossola that we are aware of. Coordinates and a short description of the samples in less-studied units are presented in Table 1. Only a few of these samples exhibit eclogite-facies assemblages unaffected by later retrograde reactions. Nevertheless, several types of textural and mineralogical evidence visible in thin section can be taken as evidence that HP metamorphism affected these mafic rocks. Observation of some combination of the following features strongly increases the likelihood of a HP record:

a) Persistence of some relics of the HP assemblage garnet-omphacite-rutile.
b) Symplectite of diopside and plagioclase or amphibole and plagioclase, which evidently replaces HP omphacite and/or garnet. Relic grains of omphacite or garnet are commonly observed in symplectite felts.
c) A rock matrix composed of fine- to very fine-grained intergrowths of amphibole and plagioclase. Considering the post-HP Barrovian metamorphism in the study area, which reached middle to upper amphibolite facies, an interpretation of these textures as partially recrystallised symplectites (see b) seems plausible.
d) Relic, resorbed garnet grains, often in combination with a kelyphitic corona rich in plagioclase and amphibole.
e) Plagioclase occurs only in garnet coronas or in symplectite domains, and apparently results from the breakdown of a former high-grade assemblage.
f) Occurrence of partially resorbed or back-reacted phengite, kyanite and/or zoisite.
g) Reaction of rutile to ilmenite and/or titanite.
h) Garnet cores incorporating numerous rutile needles and/or tiny anhedral zircon crystals. Although the exact significance of these inclusions is unclear, such cores are typically observed in HP rocks from the Central Alps.

Petrography and PT-evolution of individual samples

Thermodynamic computation of eclogites

Thermodynamic computation of rocks is challenging (e.g. Ashworth et al., 2004; Evans, 2004), in particular if the rocks are mafic (Hoschek, 2004). The most important sources of uncertainty are the reliability of thermodynamic standard state and solution data used for computation, but additional uncertainty arises from extent of equilibration on the grain or sample scale, the extent of re-equilibration along the retrograde path and the fact that phase diagrams are generally calculated for isochemical systems. The latter may be problematic when considering volatile phases like H_2O or CO_2 or samples with refractory phases like garnet. Nevertheless, thermodynamic computation has become a standard method in metamorphic petrology and is preferred by many workers over general petrogenetic grids or combinations of simple thermobarometers. Because rock samples have a specific bulk composition, isochemical phase diagrams for this composition are more appropriate for a particular sample than a general petrogenetic grid for a system like CNFMASH. Individual thermobarometers share many of the problems inherent to thermodynamic computation because they also rely on assumptions of local equilibrium, as well as on assumptions specific for each calibration (e.g. normalisation, Fe–Mg ratio, etc.). Comparison of results of different calibrations for the same thermobarometer shows that differences are often on the order of ± 50 °C and ±1–2 kbar, which is comparable to errors resulting from thermodynamic computation.

Thermodynamic computation allows two approaches to modeling petrogenesis: (1) the composition of phases in a certain domain of a sample may be used to calculate the equilibration conditions of that domain. This multi-equilibrium approach is based on the assumption that all phases in the domain were trapped in equilibrium state

Table 1 Localities (with Swiss coordinates in metres) and short descriptions of rocks preserving evidence of HP metamorphism from the Central and Western Lepontine dome. Numbers correspond to figure 1. Sources: 1–This study; 2–Collections of the Basel Museum of Natural History and the Institute of Mineralogy and Petrography, University of Basel; 3–Burri (1999); 4–Burri (2005); 5–Colombi and Pfeifer (1986); 6–Forster (1947); 7–Grandjean (2001); 8–Gräter and Wenk (1998); 9–Gutzwiler (1912); 10–Häuselmann (1997); 11–Kobe (1956); 12–Möckel (1969); 13–Pfeifer et al. (1991); 14–Tóth et al. (2000); 15–Wang (1939).

Map	Location	Sample	Coordinates		Phases			Textures					Remarks	Sources
			X	Y	Grt	Cpx	Rt	fine symp	reX symp	Rt rimmed	Rt incl.	Plag symp		
1*	Porcaresc	Porc1a	680550	121525	!	x	x	!	0	x	x	yes	Phg, Zo and Ky breakdown, Ky relics, hourglass Zo	4
2	Bordoglio	Bor2,4	696975	116960	!	!	x	!	!	x	x	yes	All stages from eclogite to amphibolite presemt	1,4,11
3		Mag286	691150	133850	!	relics	x	!	x	x	0	yes	Phg breakdown, Cpx rims around Qtz	4,8
4		Gari2	696075	119350	!	x	x	!	0	x	x	yes	Polygonal Qtz, Cpx rims around Qtz, Ky and Zo breakdown	4,11
5	Capoli	Cap6,7	699200	118840	!	!	x	!	!	x	x	yes	All stages from eclogite to amphibolite presemt	1,4,11,13
6		Big8	690525	132325	x	0	x	0	x	x	x	-	Zo breakdown, atoll Grt	4
7		Big6	690175	131525	x	x	x	0	x	x	0	yes	Hourglass Zo, Plag only where replacing Zo, carb. present	4
8		Bron6	690825	134000	0	0	x	incl. in Hbl	0	x	0	-	Strongly reX, Zo relics	4
9	Campo Tencia	Tenc1	701300	138300	x	x	x	x	x	x	(x)	yes	Most sympl is fine	4
10		Mag177	691150	133850	relics	0	x	0	x	x	0	-	Plag coronas around Grt, Bt cluster may pseudomorph Phg	4,8
11		Mag296	691530	132590	x	0	x	0	0	x	0	no	Zo breakdown to Plag, paragonite clusters	4,8
12		Vz854	704250	135450	X	Incl. in Grt	x	!	x	x	0	yes	Amp is smaragdite, Phg breakdown, hourglass Zo	2,4
13		Wurz152	703000	117270	!	!	x	!	!	x	0	yes	Amp may coexist with eclogite assemblage	2,4
14		Grü475a	690200	~130000	!	Incl. in Ky	x	!	0	x	!	yes	Ky breakdown, Zo present, Amp is smaragdite	2,4
15		Grü497	~689500	~131450	x	x	x	0	x	x	x	yes	Sympl. quite fine, Zo present, Ky partly to Stau, two Amp	2,4
16		Som8,9	694275	127120	x	0	x	0	x	x	(x)	yes	Sympl. quite fine, Bt pseudomorph after Phg?	4
17		Vz135	699500	132500	!	0	0	0	0	0	0	yes	Plag only where replacing Grt with Ep, Amp is Smaragdite	2,4
18		PD80	685960	121600	!	x	x	x	0	x	x	yes	Phg breakdown, K-rich rock	4,10
19		Alz74	685960	121600	x	0	x	0	x	0	!	yes	Grt resorption producing Pl ± Amp rim	3
20		PD74	685300	122290	x	0	x	x	x	x	0	yes	Phg breakdown, K-rich rock	4,10
21	Monteggia		702700	117300	!	x	x	!	-	-	-	-	Phg breakdown	6
22	Frunt		702400	116600	!	x	0	!	-	0	0	-	Atoll-Grt, Phg breakdown	6
23	Valeggia		~702050	~117100	!	x	x	!	-	-	x	-	Phg and Ky breakdown, Cpx rims around Qtz	6
24	Gallinee		701800	117250	!	x	x	!	-	-	x	-	1 sample with vesuvianite breakdown	6
25	Fontai		706600	117250	!	x	x	!	-	-	x	-	Phg breakdown	6
26	Cardada		704950	117400	!	x	x	!	-	-	x	-		6
27		Mont1	703300	117250	!	x	-	-	-	-	-	-	Retrogressed eclogite, no thin section	4
28	Corte della Cima		698500	118850	-	-	-	-	-	-	-	-	Retrogressed eclogite, similar to Capoli (#5)	11,13
29	Salmone		697750	118800	-	-	-	-	-	-	-	-	Retrogressed eclogite	11,13
30	Pedesen		696050	118650	-	-	-	-	-	-	-	-	Retrogressed eclogite	11,13
31	Ledrima		694200	119350	-	-	-	-	-	-	-	-	Retrogressed eclogite	11
32	Cavigliano		698760	115900	x	x	0	x	-	0	-	-	Retrogressed eclogite	5,11
33	Auression		696000	118680	x	x	0	x	-	0	-	-	Retrogressed eclogite	5,11
34	Gordemo	OS46,54	709200	115800	x	x	x	(x)	x	0	-	yes	Zo in matrix, blueish Amp in Grt	2,9,15
35	Monti di Ditto		712600	116700	-	-	-	-	-	-	-	-	Ultramafic, Chl-nests after Grt	15
36	Monti della Motta	Be9916-21	712090	116580	x	x	x	x	x	x	-	yes	Cpx tims around Qtz, one Ky relic in Grt	1,7,15
37	Alpe Repiano	Rep9702	713900	129300	x	x	x	x	0	x	x	yes	Ttn rim around Rt+Ilm, minor carbonate present	1,7
38	Alpe Arami	Be9901	718925	121050	!	!	!	(x)	0	(x)	-	yes	Rare Ky, little retrogression	1
39	Gorduno	Be9903,Ma9338	722750	119900	x	x	x	x	x	x	(x)	no	All stages from eclogite to amphibolite presemt	1,7,12,14

* Just to the west of map, !=ubiquitous, x=present, (x)=minor, 0=absent, -=unknown, reX symp=recrystallised symplectite, Rt rimmed=Rt to Ilm, Rt-incl=Rt-rich garnet cores, Plag symp=Plagio occurs only in coronas and symplectites. Mineral abbreviations cf. Kretz (1983).

and that their compositions did not change significantly afterwards. Although many arguments favour this approach (e.g. Todd and Engi, 1997) it is not trivial (Ashworth et al., 2004; Evans, 2004). (2) Isochemical phase diagrams and isopleths of mineral composition may be computed for a specific bulk composition. These diagrams can be used to infer from calculated stability fields the PT-range in which a certain mineral assemblage may have equilibrated in a rock of that composition. In addition, PT-conditions of the formation or equilibration of a mineral can be inferred using calculated isopleths for the composition of this phase. The reader is referred to Hoschek (2004) for a more detailed comparison of thermodynamic computation and conventional thermobarometry.

A recent comparison showed that significant differences in computed phase diagrams arise from the use of different software packages, thermodynamic datasets or bulk compositions (Hoschek, 2004). The author compared isochemical phase diagrams for a kyanite eclogite from the Tauern window in the Austrian Alps computed using (a) THERMOCALC (Powell et al., 1998) in combination with the THERMOCALC dataset (Holland and Powell, 1998); (b) DOMINO (de Capitani and Brown, 1987; de Capitani, 1994) in combination with an updated version of the Berman (1988; 1990) database; and (c) Perple_X (Connolly, 1990; Connolly and Petrini, 2002) in combination with the Gottschalk (1997) database. The author concludes that a preference for THERMOCALC is justified because the thermodynamic database is more recent and solid-solution models, especially for amphiboles, are more extensive. However, since Hoschek (2004) in each instance varied not only the programme, but also the thermodynamic database and solid-solution models, we consider this conclusion not entirely valid. This is illustrated by the fact that the phase diagrams calculated using THERMOCALC and Perple_X with the same database and bulk composition are remarkably similar, even if the different programmes somewhat restrict the transferability of solid-solution models (Hoschek, 2004). Using the same database and bulk system, THERMOCALC, DOMINO and Perple_X must result in almost identical phase diagrams. Nevertheless, the conclusion of the author that results of thermodynamic computation of mafic rocks should be considered with caution is certainly correct. Weaknesses are the still relatively poor standard-state and solid-solution model data for complex solution phases like amphibole and epidote, even in the most current version of the Holland and Powell (1998) database, amended with the latest solid-solution model for amphiboles (Dale et al., 2005). We note that these limitations also apply to the isochemical phase diagrams presented below, which were calculated using DOMINO (de Capitani and Brown, 1987; de Capitani, 1994) with a transferable dataset (based on Holland and Powell, 1998, details below). Future research will undoubtedly refine the datasets and solution models, and allow improvement upon the models presented here. However, we are confident that the current datasets and software are robust enough to draw qualitative and semi-quantitative conclusions. Quantitative results from isopleth computation should be regarded with reasonable caution, because errors may still be substantial.

Methods of thermodynamic computation

The reconstruction of PT-paths for metamorphic rocks is both facilitated and hampered by incomplete equilibration: domains of chemical equilibrium need to be identified. Textural relations among such domains and transitional parts of a sample may help establish the sequence of evolutionary steps. Problems and advantages of the local equilibrium approach have been discussed extensively in the literature (e.g. Ashworth et al., 2004; Evans, 2004). We use two methods to infer PT-conditions at which rocks equilibrated: (1) calculation of equilibration conditions of mineral pairs analysed by electron microprobe, using *TWQ* (Berman, 1991); (2) calculation of isochemical phase diagrams using DOMINO (de Capitani, 1994) for the system (K)CNFMASHTi. Isopleths for the components of minerals (e.g. X_{Mg} in garnet), calculated by DOMINO were used to estimate the conditions at which the minerals grew.

TWQ-calculations use an extended database of Berman (1988, update 1992) with an updated and consistent model for omphacite (Meyre et al., 1997). DOMINO calculations use the internally consistent database of Holland and Powell (HP98, 1998), with minor modifications. Ilmenite is computed as an ideal binary ilmenite-geikielite solution, and glaucophane as a one-site glaucophane – Fe-glaucophane solid-solution, with a_{glau} equal to $(X_{Mg})^3$. Following HP98, Ca-amphibole was calculated as a non-ideal tremolite–ferrotremolite–tschermakite–ferrotschermakite–pargasite–ferropargasite solid-solution. Glaucophane and Ca-amphibole solid-solutions commonly overlap in PT-space at blueschist-facies conditions. Furthermore, Ca-amphibole is predicted to unmix into two amphiboles at lower pressures. For simplicity, areas with two stable Ca-amphiboles are not separately indicated in the computed phase diagrams. H_2O saturation is assumed for all sam-

ples, which is an effective way to model the introduction of external fluids during retrogression. This assumption leads to the presence of free water vapour during prograde metamorphism, which has no additional effects on mineral modes and compositions, but allows the formation of hydrous phases upon retrogression.

A brief description of all samples is included in Table 1, as are the Swiss coordinates for each of the samples. Sample locations are also indicated in figures 1 and 2. Note that the Porcaresc locality is situated just off the map in figure 1, about 5 kilometres due west of location 18/19. Table 2 lists the whole-rock major element compositions of the samples studied in detail.

Case studies

Bordoglio

Samples from Bordoglio belong to a narrow trail of metasedimentary and mafic rocks embedded in migmatitic orthogneiss of the Orselina zone; the mafic lenses form a complete suite from nearly pristine kyanite-phengite-eclogite to almost completely equilibrated biotite-amphibolite. In addition, these samples range from coarse-grained and homogeneous, to fine-grained and laminated. Aluminium enrichment of some laminae results in abundant kyanite, which locally contains inclusions of garnet and shows unequivocal evidence of resorption. The resulting plagioclase coronas are intergrown with hercynitic spinel (Fig. 3a). Breakdown of HP phengite occurs in relatively strongly retrogressed samples, producing a domain consisting of a felt of celadonite-poor white mica (Si = 3.0–3.1 p.f.u., Fig 3b), which is armoured by plagioclase. Other phases present in this domain are anorthite-rich plagioclase, ilmenite, K-feldspar and biotite, intergrown with the plagioclase rims. Sample Bor2 is a relatively strongly retrogressed eclogite-sample containing coarse-grained garnet with inclusions of zoisite, anorthite-rich plagioclase, amphibole of pargasite to magnesiohornblende composition and clinopyroxene. Garnet cores contain abundant rutile inclusions. Garnet is generally rich in almandine, with the core slightly enriched in grossular and depleted in pyrope (Fig. 4a). The outermost rim is defined by a small increase in almandine and a small decrease in pyrope, likely related to diffusional re-equilibration or resorption.

The computed phase diagram (Fig. 5a) is relatively complicated, especially at amphibolite-facies conditions, and so only fields significant for the history of the rock are labelled. Calculated isopleth intersections for all analyses from the garnet profile indicate that growth zoning developed due to prograde consumption of glaucophane, talc and lawsonite between 2.6–3.2 GPa at 550–600 °C. The garnet core composition with slightly increased pyrope yields pressure estimates around 3.2–3.3 GPa, the intermediate section 2.6 GPa and the rim about 3.4 GPa (inset in Fig. 5b). This rather erratic path may be the result of unequal ionic diffusivity due to geologically rapid changes, leading to local differences in the effective bulk composition (i.e. domain formation). We note the absence of coesite inclusions, despite its predicted stability at the conditions derived from garnet zoning. Polycrystalline quartz aggregates do occur as inclusions in garnet, but

Table 2 Whole-rock major element compositions.

Locality	Bordoglio	Porcaresc	Capoli	Arami	Repiano	M. Motta	Gorduno
Sample	Bor2	Porc1	Cap6	Be9901	Rep9702	Be9918	Bocchio[1]
SiO_2 wt.%	48.82	47.67	43.12	48.56	44.59	49.58	48.04
TiO_2 wt.%	2.33	1.84	1.64	1.61	1.34	1.36	1.36
Al_2O_3 wt.%	16.00	19.39	16.77	15.98	13.82	14.71	14.97
Fe_2O_3 wt.%	13.86[2]	9.92[2]	15.38[2]	11.7[2]	14.22[2]	9.87[2]	2.03
FeO wt.%							8.32
MnO wt.%	0.18	0.10	0.29	0.19	0.65	0.17	0.17
MgO wt.%	5.92	6.14	9.76	7.84	8.94	8.33	9.51
CaO wt.%	8.48	10.51	12.18	10.38	11.28	11.12	11.32
Na_2O wt.%	2.74	2.55	1.01	3.73	1.47	4.59	3.11
K_2O wt.%	0.19	0.74	0.02	0.04	0.33	0.44	0.06
P_2O_5 wt.%	0.29	0.16	0.07	<0.01	0.02	0.22	0.12
LOI wt.%	0.46	0.32	–0.77	–0.13	0.63	0.39	0.44
SUM wt.%	99.27	99.34	99.47	99.90	97.29	100.78	99.45

[1] Average of 5 eclogites from Gorduno, compiled by Bocchio et al. (1985)
[2] Fe_{tot} analysed as Fe_2O_3

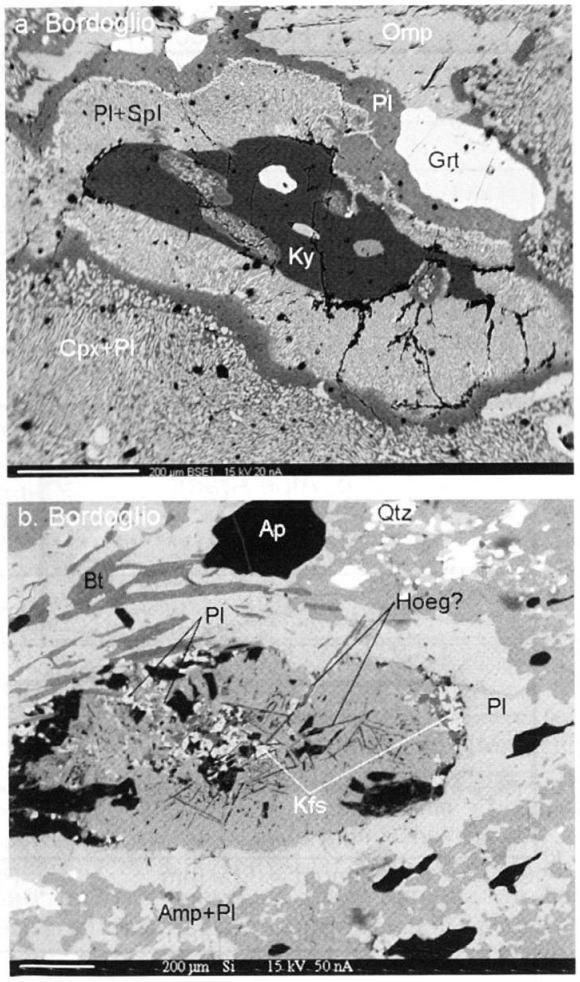

Fig. 3 (a) BSE-image of kyanite decay in Bordoglio sample Bor4. The partially resorbed kyanite grain is surrounded by a plagioclase-spinel corona. A second chemically zoned corona of plagioclase, devoid of spinel, rims the inner corona. Note partially back-reacted omphacite, that has decayed to a symplectite of Di-rich clinopyroxene and plagioclase (see also inclusion in kyanite). Phases included in kyanite are omphacite, rutile and garnet. (b) Si X-ray map of reaction texture in sample Bor2, probably related to the breakdown of phengite. An inner core, mainly consisting of low-Si muscovite, plagioclase, K-feldspar and possibly hoegbomite (Hoeg) needles is rimmed by a corona of plagioclase. Biotite is also present in the upper left of the texture. The texture is surrounded by a recrystallised amphibole-plagioclase symplectite. All mineral abbreviations in figures, tables and text according to Kretz (1983).

the typical palisade texture and surrounding radial cracks (Chopin, 2003) are not observed. However, quartz inclusions are concentrated in the inner parts of garnet, which may have formed below the quartz-coesite boundary. The HP mineral assemblage Grt+Phg+Cpx+Qtz+Rt is stable at conditions above ~650 °C and ~2.1 GPa.

The retrograde path is associated with the consumption of garnet and omphacite to form plagioclase and amphibole, at conditions below 1.8 GPa. The relatively extensive retrogression suggests that fluid must have infiltrated the rock during decompression. Breakdown of phengite started probably at ca. 1.1 GPa, followed by growth of ilmenite at around 1.0 GPa. A final PT-point along the path is the Barrovian overprint of this area at conditions of ~630 ± 20 °C and 0.6 ± 0.05 GPa, estimated by Todd and Engi (1997).

Porcaresc

The mafic lens of Porcaresc is associated with metapelites and large masses of granitic orthogneiss. Samples show complex reaction textures indicative of breakdown of phengite, kyanite, zoisite, garnet and omphacite. Kyanite, typically rounded due to partial resorption, is surrounded by anorthite-rich plagioclase, which becomes richer in albite with increasing distance from kyanite (see also Nakamura, 2002). Phengite has broken down to form aggregates of acicular biotite and plagioclase (Fig. 6). Garnet is typically rimmed by plagioclase and amphibole, and the cores of several grains contain ubiquitous fine rutile needles. Zoisite (Xpist = 0.1) is usually relatively coarse-grained, appears partially resorbed and exhibits characteristic hourglass structures (Fig. 6b). Inclusions of kyanite, garnet and clinopyroxene suggest that zoisite crystallised along the exhumation path. Omphacite breakdown led to formation of a globular symplectite of diopside-rich clinopyroxene, amphibole and plagioclase. Larger poikilitic magnesiohornblende to edenite amphiboles with inclusions of zoisite, kyanite, phengite, rutile and garnet overgrow the older matrix. Whether amphibole was part of the HP assemblage remains unclear from petrographic inspection, but the presence of kyanite argues against it because amphibole and kyanite coexist only in a small PT-area at water-saturated conditions. Quartz is often rimmed by Al-poor clinopyroxene and rutile is often partially replaced by ilmenite. Accessory phases are pyrite and apatite. Analysed garnet profiles are somewhat irregular, but generally depict a decrease in pyrope and an increase in almandine from core to rim (Fig. 4b). A plateau between core and rim of the garnet shows the highest pyrope content ($X_{Prp} > 0.32$).

Due to the lack of inclusions in garnet (except for rutile), the phase diagram provides few constraints on the prograde PT-path (Fig. 7a). According to calculated garnet-isopleths, garnet-zoning indicates exhumation from 3.7 to 2.3 GPa, followed by burial to 2.8 GPa (see inset in figure 7b). Core compositions indicate extremely high pressures of around 3.7 GPa at 670 °C, mainly determined by the high X_{Prp}. However, we infer that

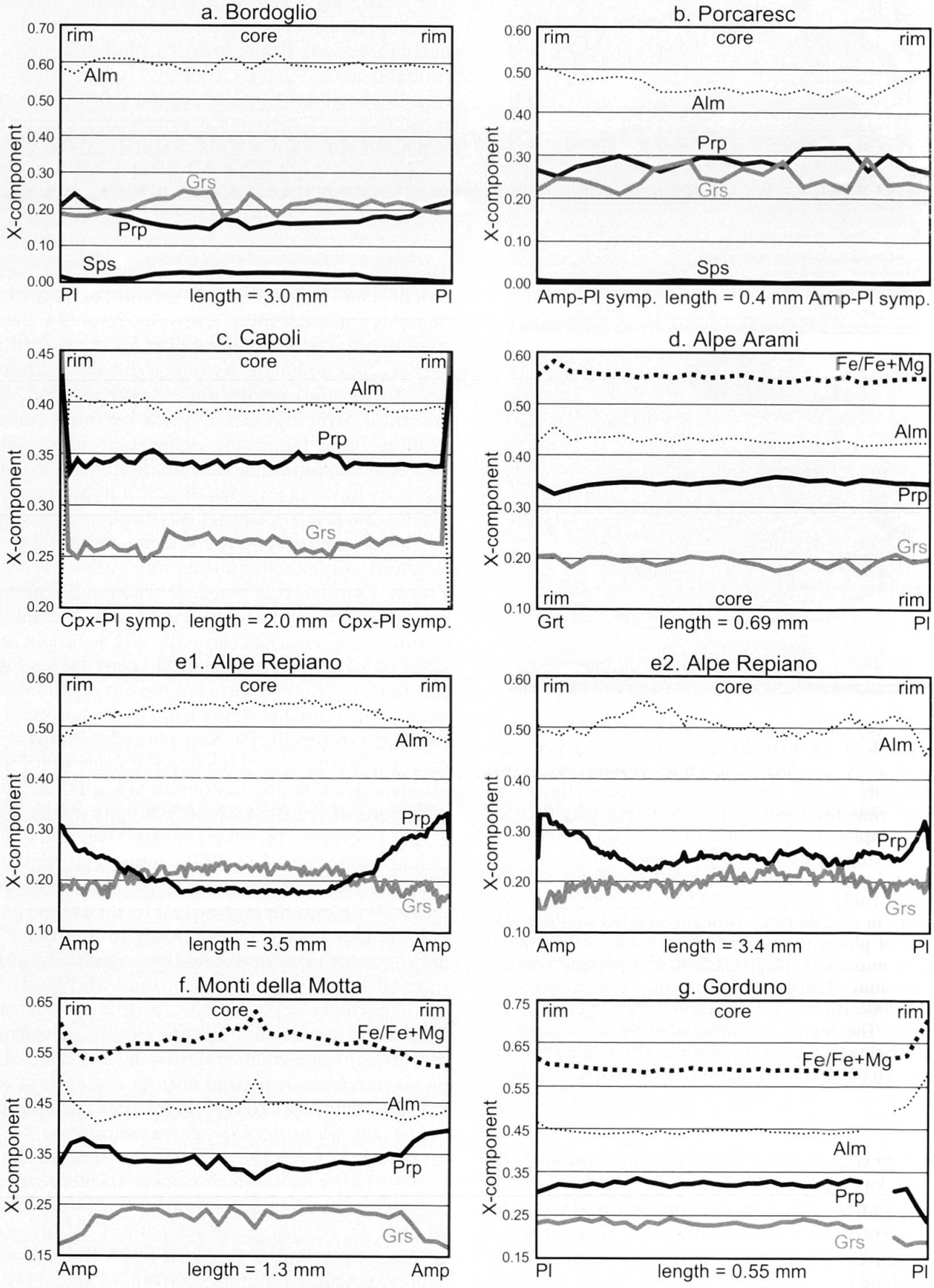

Fig. 4 EMP-element profiles through garnet. Profile length and neighbouring phases are indicated below each graph. "Symp." designates symplectite. See text for discussion. (a) Bordoglio sample Bor2. (b) Porcaresc sample Porc1. (c) Capoli sample Cap6. (d) Alpe Arami sample Be9901. (e1 and e2) Alpe Repiano sample Rep9702. (f) Monti della Motta sample Be9917. (g) Gorduno sample Ma9338.

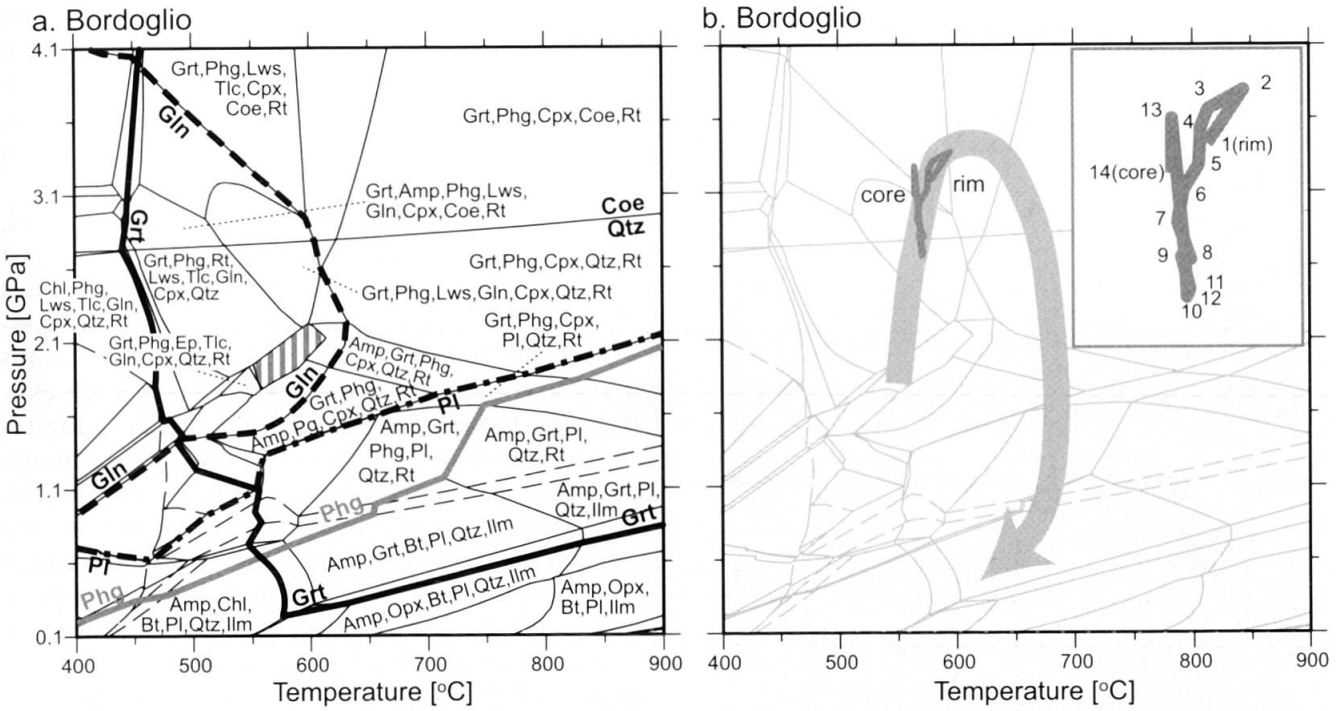

Fig. 5 (a) Computed phase relations for Bordoglio sample Bor2 in the system KCNFMASHTi, assuming H_2O-saturation and QFM-buffering. Vertically striped area denotes presence of zoisite. Thick black line = garnet, thick dashed line = glaucophane, dash-dot line = plagioclase, grey line = phengite, thin dashed lines = ilmenite-rutile-titanite. Only assemblages of importance for this study are marked. (b) Thin grey line indicates intersections of garnet isopleths using the garnet compositions along the profile in figure 4a. The garnet analyses were normalised to Alm-Prp-Grs compositions, not considering Mn. Inset is enlargement of the PT-path derived from garnet zoning. Thick grey arrow indicates approximate PT-path for the sample. See text for further discussion.

the very high pressure estimates are erroneous and result from the former presence of a high-Mg precursor like glaucophane, chloritoid or lawsonite, buffering the local chemical bulk system. Carlson (2002) recently reported such sample-scale disequilibrium for certain elements in garnet. We therefore suggest that garnet growth occurred along the prograde path between 2.3–2.8 GPa around 620 °C (inset in Fig. 7b). In detail, the path appears rather complicated, which may be related to (1) local fluctuations in effective chemical bulk or (2) different episodes of burial and exhumation. Garnet growth at the inferred conditions is related to a major change in phase relations like Gln + Lws = Grt + Omp + Qtz + H_2O, probably followed by Lws = Grt + Omp + Ky + Zo + H_2O.

The HP assemblage Grt + Ky + Omp +Qtz + Phg + Rt ± Zo is marked in Fig. 7a by a dark shading combined with vertical stripes (overlap of kyanite and zoisite fields). The diagram does not provide an upper limit to the temperature during HP metamorphism. Assuming temperatures not much in excess of 700 °C for the HP stage, minimum pressures for this assemblage are 1.9 to 2.1 GPa. Breakdown of primary omphacite during decompression occurred when the stability limit of plagioclase was encountered at approximately 1.7 GPa (at 700 °C). Phengite breakdown producing biotite and plagioclase occurred at around 0.8–0.9 GPa and 650–700 °C, also constrained by the absence of K-feldspar from all samples. A final constraint is obtained from the regional isograd pattern of Barrovian metamorphism (Todd and Engi, 1997), which at Porcaresc attained ~635 ± 20 °C and 0.67 ± 0.05 GPa.

Capoli

The outcrop of the mafic-ultramafic body of Capoli is a few hundred metres long and wide; it has an ultramafic core and several mafic bodies at the rim (Kobe, 1956; Pfeifer, et al., 1991). The mafic-ultramafic body is surrounded by migmatitic orthogneiss, and several smaller lenses occur along strike immediately to the west. The samples investigated range from completely preserved eclogites to variably retrogressed amphibolites. Retrogression led to extensive development of clinopyroxene–plagioclase or amphibole–plagioclase symplectites, whereas other samples show only the stable amphibolite-facies assemblage (Amp + Pl + Qtz + Ttn/Ilm). Three types of retrograde reactions are observed (Fig. 8): 1) Formation of an

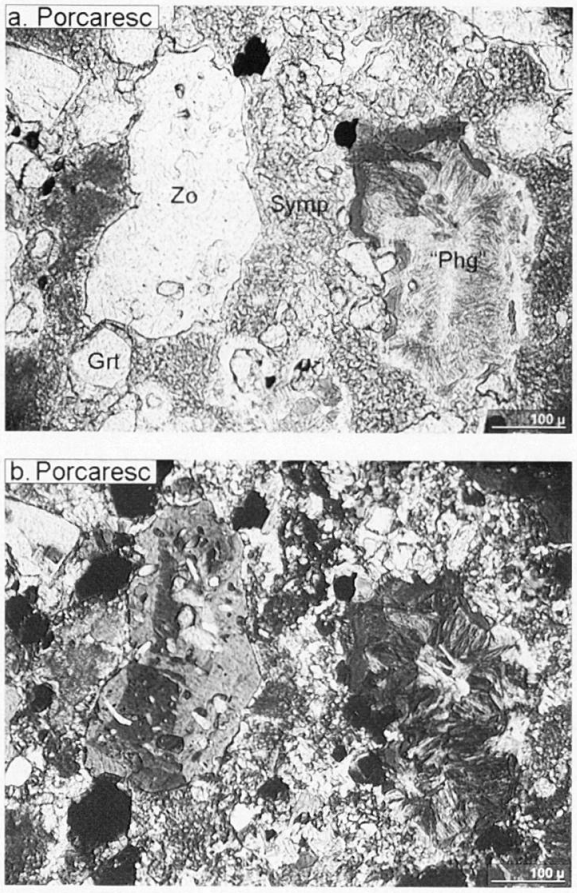

Fig. 6 Photomicrograph of reaction textures in thin section of Porcaresc sample Porc1. Note phengite breakdown domain ("Phg"), resorbed shape and hourglass structure in zoisite. Symp denotes clinopyroxene-amphibole-plagioclase symplectite. (a) Plain polarised light. (b) Cross-polarised light.

amphibole rim of a few to several tens of micrometres along garnet-clinopyroxene and garnet-garnet grain boundaries. 2) Formation of plagioclase-clinopyroxene symplectites along clinopyroxene-clinopyroxene grain boundaries. 3) Formation of ilmenite at the expense of rutile grains in the matrix. The composition of clinopyroxene varies from omphacite in well-preserved grains, to diopside-rich compositions in the symplectite. Omphacite is generally homogeneous in composition, and since X_{Na} and X_{Al} on the M-site almost coincide, Tschermaks- or aegirine-substitutions are apparently subordinate to the jadeite component. Estimations of ferric iron (calculated according to Droop, 1987) agree with the very low aegirine content. Amphibole occurs as inclusions in garnet as well as along garnet grain boundaries. The composition of inclusions varies from magnesiohornblende to pargasite, whereas retrograde amphibole ranges between pargasite and edenite. Additional inclusions in garnet are omphacite (identical composition as matrix grains), as well as a few grains of zoisite (X_{pist} = 0.1), allanite, pyrite and chalcopyrite. Garnet cores are riddled with inclusions of rutile needles. Garnet shows essentially flat zoning profiles in major elements (Fig. 4c), in which Fe/Mg-ratios increase slightly from 1.1–1.15 in the core to 1.25–1.45 at the rims.

Inclusions of amphibole and zoisite in garnet, as well as the absence of quartz inclusions suggest that the subduction trajectory was relatively hot (Fig. 9a), but the prograde PT-path is not well constrained. Using *TWQ*, the eclogite-facies assemblage Grt + Omp + Rt allows only a rough estimate of temperatures reached during eclogite-facies metamorphism, based on Mg/Fe exchange between coexisting garnet and pyroxene grains. An estimate of the peak pressure requires the presence of phengite and quartz/coesite, which are absent due to the potassium- and silica-poor bulk chemical composition of this rock (Table 2). Combining calculated phase relations with estimated *TWQ* temperatures for garnet-omphacite rim pairs from sample Cap6, minimum conditions of 750 °C at 2.0 GPa are obtained (Fig. 9b). The temperature-estimate obtained using the phase diagram and garnet isopleths computed with DOMINO coincides with the calculated *TWQ*-equilibrium. This indicates that the effective bulk composition did not significantly deviate from the bulk rock composition and that chemical fractionation due to garnet-growth is unimportant (cf. Konrad-Schmolke et al., 2005). This inference is supported by the relatively flat garnet zoning pattern, which likely results from continuous recrystallisation of garnet in the eclogite facies. The composition reflects the ambient conditions at

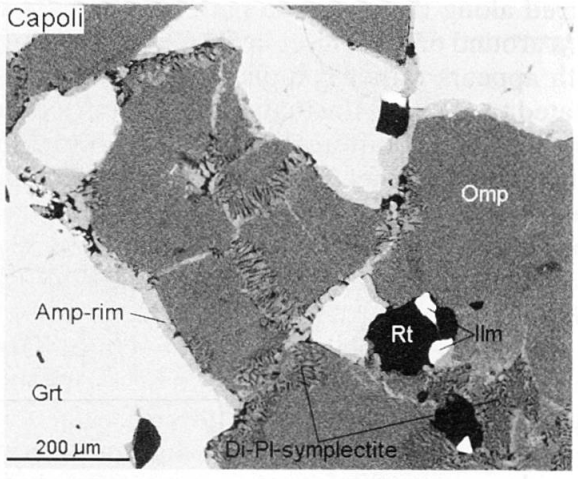

Fig. 8 X-ray map for Fe in Capoli sample Cap7. The map shows products of incipient retrograde reactions during decompression. Amphibole rims line Grt-Grt and Grt-Cpx grain boundaries. Fine-grained symplectites of Di-rich clinopyroxene and plagioclase occur along Grt-Cpx and Cpx-Cpx grain boundaries.

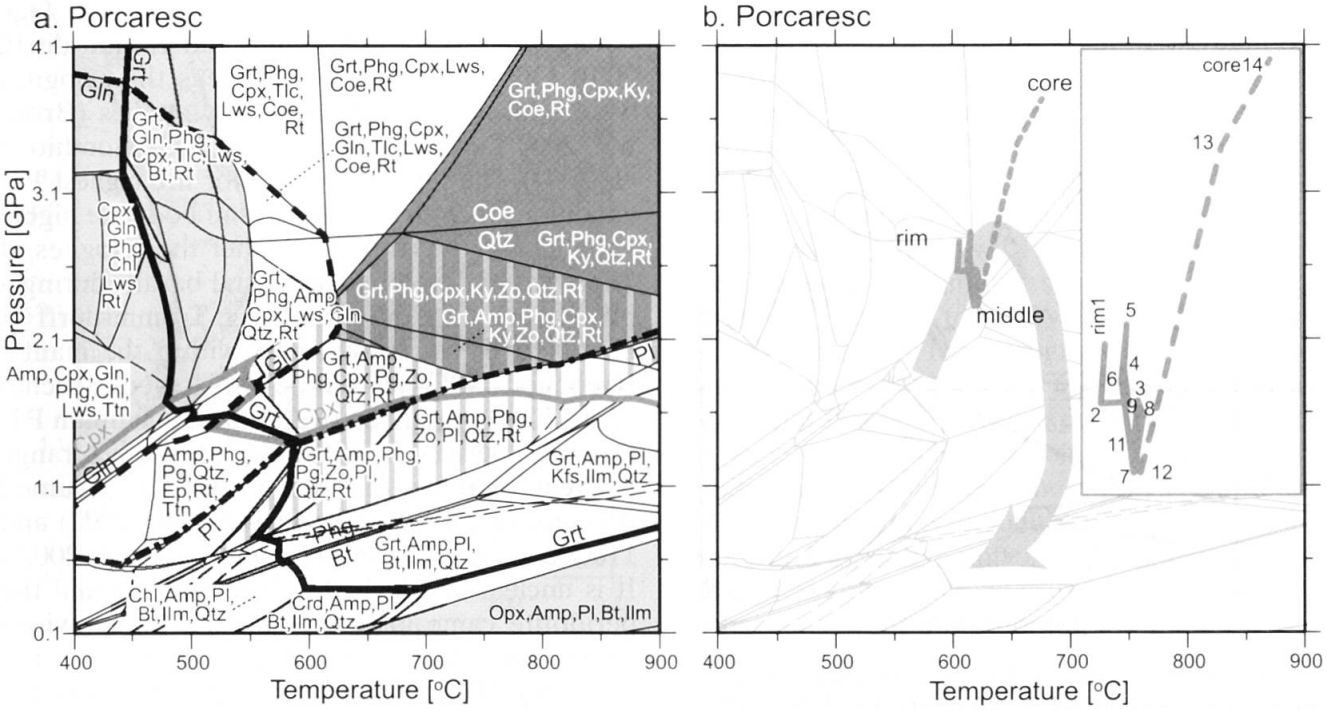

Fig. 7 (a) Computed phase relations for Porcaresc sample Porc1 in the system KCNFMASHTi, assuming H_2O-saturation and QFM-buffering. Vertically striped area denotes presence of zoisite, light grey shading absence of quartz/coesite, dark grey shading presence of kyanite. Thick black line = garnet, thick dashed line = glaucophane, dash-dot line = plagioclase, grey line = clinopyroxene, thin dashed lines = ilmenite-rutile-titanite. Only assemblages of importance for this study are marked. (b) Thin grey line indicates intersections of garnet isopleths using garnet compositions according to the analysed garnet profile in Fig. 4b. Inset is enlargement of the PT-path derived from garnet zoning. Thick grey arrow indicates approximate PT-path for the sample. See text for further discussion.

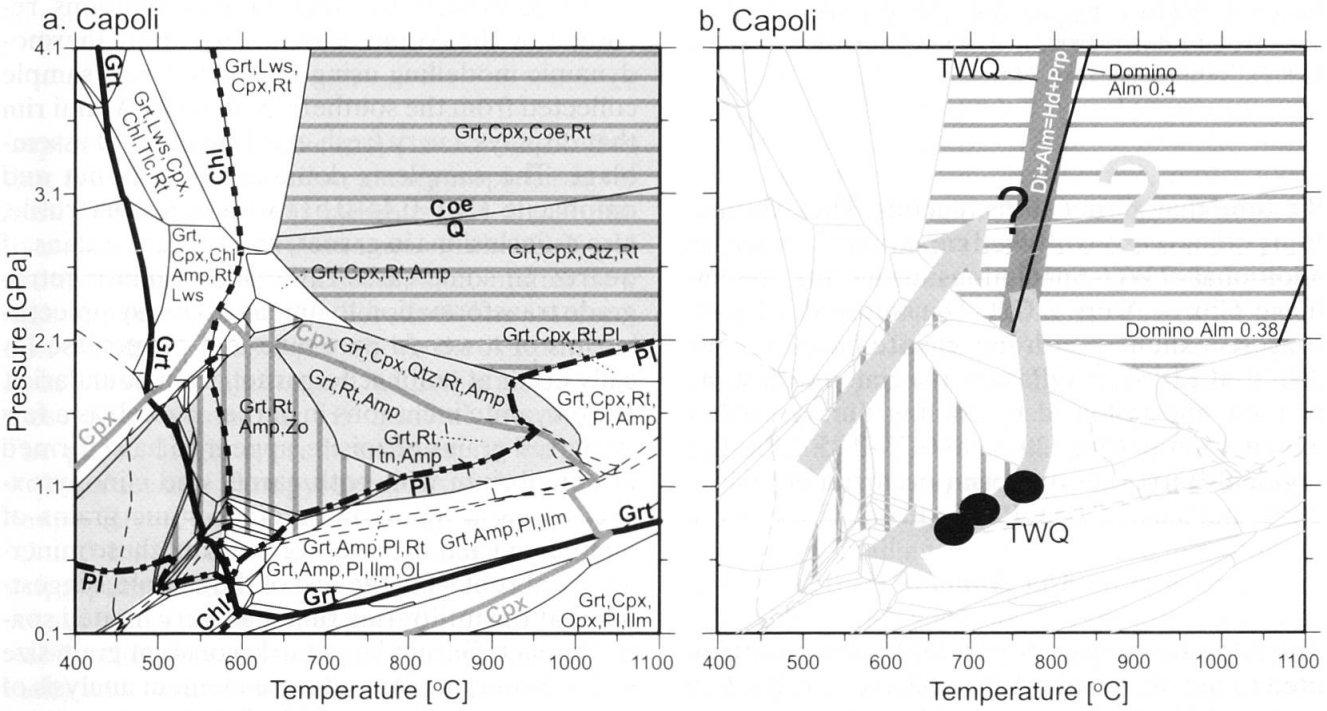

Fig. 9 (a) Computed phase relations for Capoli sample Cap6 in the system CNFMASHTi, assuming hydrous fluid saturation and QFM-buffering. Grey shading indicates presence of quartz or coesite (very low modal abundance at eclogite conditions), vertical stripes the presence of zoisite, and horizontal stripes the eclogite-facies field with the assemblages Grt+Cpx+Rt+Qtz/Coe. Thick black line = garnet, thick grey line = clinopyroxene, dash-dot line = plagioclase, thick dashed line = chlorite, thin dashed lines = ilmenite-rutile-titanite. (b) TWQ-results (dark shaded band and black ellipses) and calculated isopleths for almandine (black lines) using Domino. Grey arrows indicate approximate PT-path for the sample. The maximum pressure reached is not constrained. See text for further discussion.

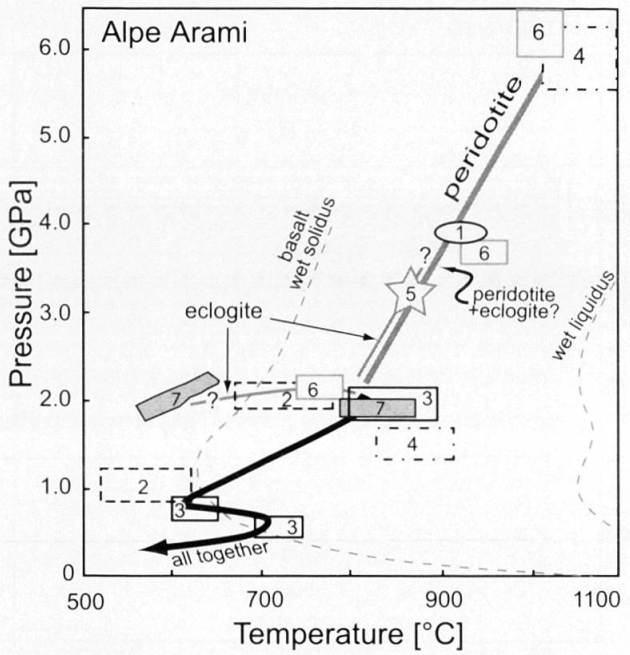

Fig. 10 Compilation of PT data obtained from the Alpe Arami body from the literature. Black line represents common trajectories of peridotite and eclogite. The thick black, continuous line is the path from common equilibration of eclogite and peridotite at ~2.0 GPa and ~800 °C down to the amphibolite facies (e.g. Brenker and Brey, 1997; Brouwer, 2000). The thick grey line indicates the inferred path of the peridotite; possible interpretations for the eclogite are shown as thin grey lines. Numbered boxes represent data from the literature: 1: Ernst (1981), 2: Brenker and Brey (1997), 3: Brouwer (2000); 4: Paquin and Altherr (2001); 5: Nimis and Trommsdorff (2001), 6: Dobrzhinetskaya et al. (2002), 7: this study (Fig. 11).

the time that garnet stops reacting. The exhumation path is reasonably well constrained, based on additional *TWQ*-calculations using the assemblage Cpx + Amp + Grt. The inferred PT-path suggests exhumation from eclogite facies to 750–800 °C at 1.05–1.15 GPa was associated with some heating, and followed by cooling during further exhumation to 670–720 °C at 0.75–0.85 GPa. The regional Barrovian overprint occurred at ~645 ± 20 °C and 0.64 ± 0.05 GPa (Todd and Engi, 1997).

Alpe Arami

The Alpe Arami garnet peridotite body is attributed to the Mergoscia-Arbedo Zone (e.g. Bächlin et al., 1974) and is surrounded by a discontinuous rim of eclogite (e.g. Möckel, 1969; Ernst, 1981). The metamorphic evolution of this composite has been the subject of numerous recent studies, after an initial report of extremely high pressure recorded in the olivine microstructure of the peridotite (Dobrzhinetskaya et al., 1996). Most subsequent work has focussed on the peridotite (e.g. Brenker and Brey, 1997; Nimis and Trommsdorff, 2001; Olker et al., 2003), whereas the eclogites were addressed in relatively few studies (Brouwer, 2000; Dobrzhinetskaya et al., 2002; Bocchio et al., 2004). The reported values for the highest PT-conditions recorded by the Arami body are highly variable and the issue of whether the eclogites of Alpe Arami developed as crustal basalts during a pre-Alpine stage of rifting (e.g. Trommsdorff et al., 2000) or as partial melts within the mantle (Gebauer, 1996) has not been resolved. Bocchio et al. (2004) present an overview of maximum PT-estimates derived from the eclogites, which range between extremes of 691 ± 31 °C at an assumed pressure of 2.0 GPa (Woodland et al., 2002) and 1100 °C at 7.0 GPa (Dobrzhinetskaya et al., 2002). It is unclear at which stage the eclogite and the peridotite came in direct contact, but previous studies agree that both rock types underwent major re-equilibration between 3 and 2 GPa at 800–850 °C (Fig. 10). After this equilibration, eclogite and peridotite reflect identical exhumation histories. HP metamorphism is followed by cooling during decompression and a stage of Barrovian reheating around 29 Ma (Köppel et al., 1981) at temperatures of 750–800 °C at a pressure around 0.7 GPa in this part of the metamorphic dome (Engi et al., 1995).

To determine the highest PT-conditions recorded by the Arami eclogites, we apply thermodynamic modelling using DOMINO to a sample collected from the southern part of the Arami rim that displays a very fresh eclogitic mineral assemblage. The sample is dominated by garnet and omphacite (X_{Jd}=0.44–0.51) with accessory rutile, also as inclusions in garnet, and very few grains of quartz. In some cases rutile shows minor retrograde transformation to ilmenite. Thin symplectitic rims of lower-Jd pyroxene and plagioclase locally occur at omphacite-garnet grain boundaries. Rare kyanite inclusions in garnet, as well as a few dispersed grains of zoisite, appear to have formed in equilibrium with both garnet and clinopyroxene. Along a quartz-lined crack some grains of apatite and allanite have formed, but these minerals are absent from the rest of the sample, suggesting that the infiltrating fluid had very limited spatial impact. Garnet has a fairly constant grain size (0.2–0.5 mm); major and trace element analysis of garnet in this sample yields flat zoning patterns with $Alm_{42-44}Grs_{22-26}Prp_{32-34}$ (Fig. 4d, Brouwer et al., submitted).

The phase diagram and garnet isopleths computed for this sample (Fig. 11) indicate that its Grt + Omp + Rt + Qtz mineral assemblage equilibrated at ~835 °C and 1.9 GPa. This coincides with the

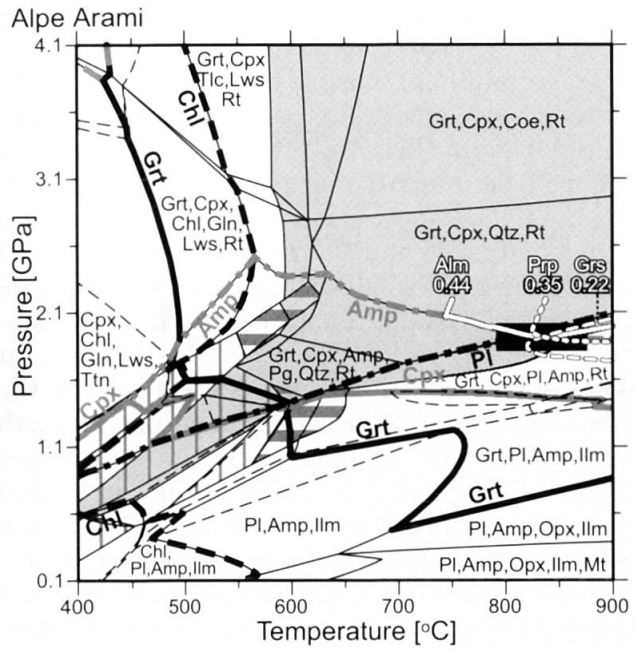

Fig. 11 Computed phase relations for Arami sample Be9901 in the system CNFMASHTi, assuming fluid saturation and QFM-buffering. The black box marks the intersection of the garnet isopleths (white lines). Grey shading indicates presence of quartz or coesite (very low modal abundance at eclogite conditions), horizontal grey stripes the presence of zoisite, and vertical grey stripes the epidote stability field. Thick black line = garnet, thick grey line = clinopyroxene, black dash-dot line = plagioclase, grey dash-dot line = amphibole, thick black dashed line = chlorite, thin dashed lines = ilmenite-rutile-titanite.

isopleth for X_{Jd}=0.50 in clinopyroxene, indicating that the estimate based on garnet isopleths is robust. The computations indicate that due to the overall Na content of this sample (Table 2) X_{Jd} of clinopyroxene never reaches 0.52, no matter how high the pressure of equilibration. The intersection of the isopleths is just above the Amp-in and Pl-in curves, in agreement with the absence of these phases from the HP mineral assemblage. The phase diagram predicts zoisite to be stable with garnet and clinopyroxene, as well as Gln + Amp + Rt ± Qtz, in a small field between 550–625 °C and 1.8–2.3 GPa (upper field with horizontal stripe pattern in Fig. 11). This suggests that the Arami eclogites were subducted into the zoisite stability field (i.e. did not crystallise from a mantle melt) and underwent near-isobaric heating prior to equilibration of the HP mineral assemblage Grt + Omp + Rt + Qtz. However, because of uncertainties involving thermodynamic models for amphibole and epidote minerals, as well as the ferric iron content of the rock, we do not use the modelling results for zoisite as a rigid constraint for the prograde path of the sample. Observations and modelling do not exclude the possibility that the rock experienced much higher PT-conditions in the eclogite field, but in that case any record was obliterated by continuous recrystallisation of the HP assemblage, resulting in a homogeneous distribution of major and trace elements in garnet. The absence of kyanite from the phase diagram, in combination with its occurrence as small inclusions in our sample, suggests that kyanite formed in response to local variations in effective bulk composition. The retrograde trajectory is not constrained by the minerals in this sample; we assume that this sample followed the path outlined in the compilation for the composite Alpe Arami body (Fig. 10). Consistent thermodynamic modelling of this Arami eclogite unfortunately does not produce a definitive upper limit to the metamorphic pressure that affected these rocks or additional constraints on the retrograde path. However, equilibration of the eclogite is constrained at ~835 °C and 1.9 GPa, at the lower-pressure end of the plethora of previous estimates.

Alpe Repiano

The eclogite lens at Alpe Repiano is an isolated and fault-bounded fragment at the eastern margin of the Cima Lunga unit and overlain by gneisses of the Maggia nappe. It is likely an isolated sliver of Cima Lunga. The sample selected for analysis is a fairly coarse-grained mafic rock, in which garnet ranges in size from 2 to 5 mm (Fig. 12a). Garnet is surrounded by a dominantly symplectitic matrix of Cpx + Amp + Pl + Rt. Some garnet grains show symplectite rims, in turn locally replaced by granoblastic amphibole. Matrix rutile shows limited marginal transformation to ilmenite, and a thicker rim of titanite. Most garnet grains contain zones with numerous rutile inclusions, and some inclusions of quartz, amphibole or epidote are present. A single large inclusion of omphacite (X_{Jd}=0.20) has been reported by Grandjean (2001), who noted that this inclusion is accompanied by amphibole and quartz and shows signs of exsolution, all of which indicate retrogression. Rare small and rounded zircon inclusions (a few μm across) are concentrated in garnet cores (Fig. 12b), which suggests that they developed by exsolution from the garnet. Garnet can incorporate significantly more zirconium at high grade than at low grade (Fraser et al., 1997; Degeling et al., 2001; van Westrenen et al., 2001; Tomkins et al., 2005), hence Zr may exsolve from garnet upon cooling and/or decompression. Cathode-luminescence imaging could support this hypothesis if the zircon CL-patterns do not show the oscillatory zoning of igneous zircon, but a definitive distinc-

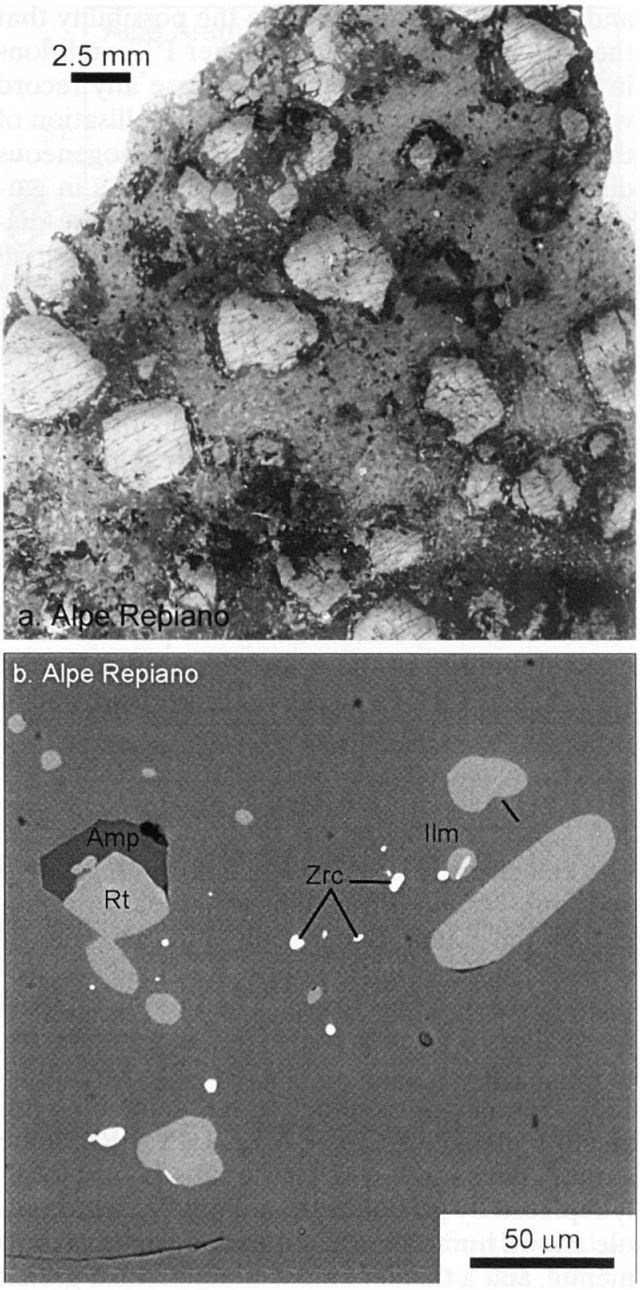

Fig. 12 (a) Photomicrograph of Alpe Repiano sample Rep9702. Garnet porphyroblasts are surrounded by a rim of granoblastic amphibole in a matrix of mostly clinopyroxene-plagioclase symplectite. (b) BSE image of inclusions of rutile and exsolved zircon in a 5 mm-sized garnet in Rep9702.

tion between entrapped metamorphic zircon and exsolution can not be made on the basis of CL-images. Garnet is strongly zoned in major and trace elements (Brouwer, et al., submitted). Garnet compositions and zoning patterns vary from grain to grain, determined in part by how garnet has been cut in the thin section. In garnet cores the composition is $Alm_{56-87}Grs_{21-24}Prp_{18-23}$, whereas the rim composition is $Alm_{45-49}Grs_{18-24}Prp_{27-36}$ (Fig. 4e1–2). Trace element zoning patterns mimic the shape of major element zoning, with cores enriched in the HREE relative to garnet rims.

PT-conditions recorded by this rock were estimated using isopleths for garnet composition in a phase diagram (Fig. 13a). The diagram is complicated in the amphibolite facies (around 550 °C and 0.6 GPa), where small stability fields of chloritoid, margarite and staurolite are predicted. At lower pressure, a small stability field for cordierite is predicted. Clinopyroxene is expected to be stable above ~1.3 GPa. The prograde evolution of the Repiano sample is only constrained by the presence of epidote inclusions in garnet. Isopleth intersections for the core composition of garnet plot at ~575 °C and 2.7 GPa and the predicted mineral assemblage at the onset of garnet growth is Grt + Cpx + Amp + Gln + Lws + Qtz + Rt. Inclusions of clinopyroxene, amphibole, quartz and rutile are indeed present in garnet cores, but glaucophane and lawsonite have not been found in this sample. The absence of lawsonite and glaucophane may indicate that both phases have completely reacted out, or that the amount of H_2O included in the model bulk assemblage is an overestimate. Thermodynamic data for glaucophane and mixing models for complex sodic amphiboles remain dubious, leaving the significance of this apparent discrepancy unclear. The garnet rim composition fails to produce an intersection of the calculated isopleths, but decreasing values of Fe/(Fe+Mg) towards garnet rims (Fig. 4e) suggest that the ambient temperature rose by about 100 °C during garnet growth (Fig. 13b). In most grains the grossular content decreases from core to rim, which suggests a pressure-increase during heating. There are no indications for UHP metamorphism in the form of polycrystalline quartz aggregates or radial cracks around inclusions in HP minerals, although at the estimated maximum pressure for the Alpe Repiano body coesite is stable. Combined petrography, phase diagram and isopleths for almandine and pyrope suggest that the stable mineral assemblage was Grt + Cpx + Qtz + Rt ± Amp at conditions around 625–675 °C and 2.8–3.1 GPa at the time of garnet rim growth.

Previous work and the new phase diagram (Fig. 13) provide some quantitative constraints on the evolution of the Repiano sample after HP metamorphism. The isopleth for X_{Jd}=0.2 is located at T>800 °C and 1.5–1.7 GPa, which puts the equilibration of this grain solidly on the exhumation path, but at temperatures markedly higher than the conditions of garnet growth. Decompression is mainly documented by the growth of calcic amphibole and plagioclase at the expense of garnet and pyroxene. Grandjean (2001) applied amphibole-plagioclase thermometry (cf. Holland

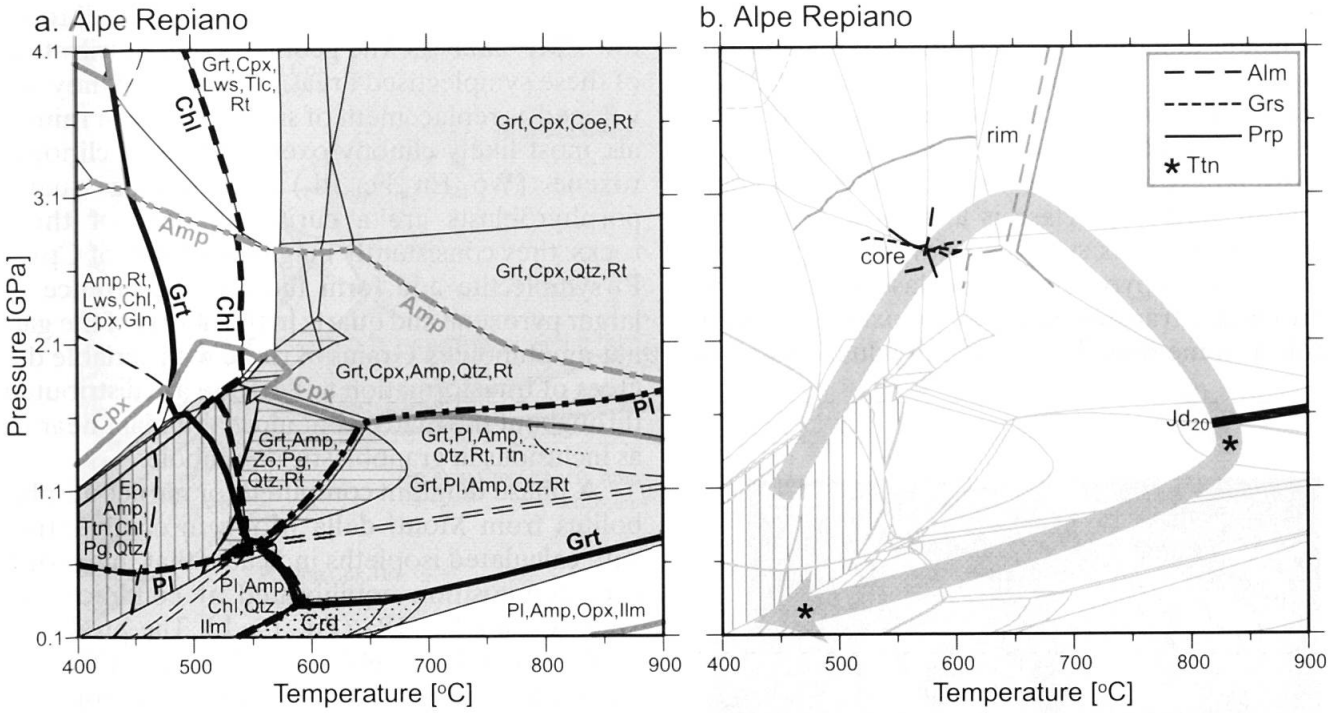

Fig. 13 (a) Computed phase relations for Alpe Repiano sample Rep9702 in the system CNFMASHTi, assuming fluid saturation and QFM-buffering. Grey shading indicates presence of quartz or coesite (very low modal abundance at eclogite conditions), horizontal stripes the presence of zoisite, vertical stripes denote epidote and the dotted pattern indicates the presence of cordierite. Thick black line = garnet, thick grey line = clinopyroxene, black dash-dot line = plagioclase, grey dash-dot line = amphibole, thick black dashed line = chlorite, thin dashed lines = ilmenite-rutile-titanite. (b) Black isopleths, calculated using DOMINO, reflect garnet core compositions, grey isopleths the rims. X_{Jd}=0.20 is also indicated. Stars indicate the stability of titanite; titanite rims around Rt+Ilm most likely developed at temperatures below 500 °C during the late stages of exhumation. Grey arrow indicates approximate PT-path for the sample.

and Blundy, 1994) as well as modelling of a Grt + Amp + Plg kelyphitic assemblage to deduce that conditions of 800–875 °C were recorded during exhumation between 1.1 and 0.8 GPa. Finally, the regular occurrence of the sequence Rt ⇒ Ilm ⇒ Ttn reflects later stages of exhumation. Barrovian conditions for this locality were estimated at ~660 ± 20 °C and 0.59 ± 0.05 GPa (Todd and Engi, 1997).

Monti della Motta

At Monti della Motta in the Southern Steep Belt, several mafic layers and lenses are enclosed in a composite of migmatitic orthogneisses and some paragneiss of the Mergoscia-Arbedo zone (Grandjean, 2001). The size and geometry of the lenses is poorly constrained, because the outcrops are located on a forested slope northeast of Locarno. Amphibolite layers consist of foliated dark green to black amphibolite gneisses, whereas greenish-grey garnet-amphibolite lenses are least retrogressed in their cores and preserve a weak HP foliation, which differs in orientation between lenses. At the rim of garnet-amphibolite lenses garnet has largely been replaced by amphibole and plagioclase, and the foliation aligns with the regionally dominant E–W foliation of the SSB. In thin section, garnet amphibolite samples are dominated by partially resorbed 0.5–2 mm garnet porphyroblasts in a matrix with various types of symplectite, and granoblastic calcic amphibole (Fig. 14a). Garnet is somewhat zoned in its major element composition, with $Alm_{45-49}Grs_{21-24}Prp_{31-33}$ in the core and $Alm_{41-43}Grs_{17-20}Prp_{38-40}$ at the rim. Grossular produces a fairly flat plateau, with marked decrease near the rim, whereas the almandine and pyrope components show a more continuous, slightly erratic pattern, especially obvious from Fe/(Fe+Mg) (Fig. 4f). The sharp increase in Fe/(Fe+Mg) at one rim is attributed to diffusional resetting and resorption during regional Barrovian metamorphism. Garnet porphyroblasts contain ubiquitous rutile needles, as well as some small (up to 10 μm diameter) rounded inclusions of zircon, which are concentrated in garnet cores. As in the Repiano sample, we interpret the zircon inclusions to result from exsolution during decompression. Closer to the rims inclusions of quartz, amphibole, idiomorphic rutile and sparse epidote occur. A single grain of kyanite,

accompanied by amphibole, was identified as an inclusion in garnet (Grandjean, 2001). Small garnet grains are generally devoid of inclusions. Garnet is usually surrounded by a corona of fine intergrowths of edenitic amphibole and plagioclase (An_{40-60}); towards the outside these become coarser, and plagioclase is less calcic (An_{20}, Fig. 14a). Most matrix symplectite is made up of fine-grained clinopyroxene-plagioclase intergrowths, with minor transformation of pyroxene to amphibole at some rims (Fig. 14b). Individual crystals of both pyroxene and plagioclase are too small to allow EMP-analysis. The geometry and distribution of these symplectised areas suggests that they developed as replacement of single precursor minerals, most likely clinopyroxene. Atolls of clinopyroxene ($Wo_{44}En_{36}Fe_{14}Jd_5$) surrounding quartz porphyroblasts are a curious feature of these rocks; they consistently neighbour zones of Cpx + Pl symplectite and form the only occurrence of larger pyroxene and quartz in the matrix of the garnet-amphibolites. Grains of rutile with variable degrees of transformation to ilmenite are distributed throughout the matrix, but most abundant near or as inclusions in granoblastic amphibole.

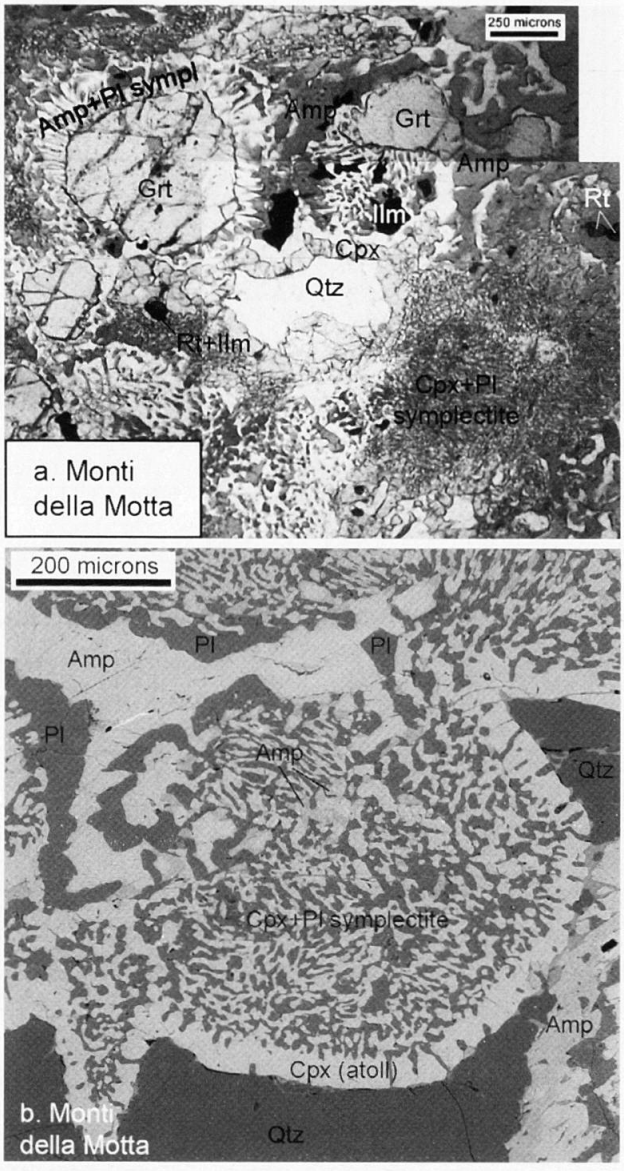

Fig. 14 (a) Photomicrograph of Monti della Motta sample Be9918, showing partially resorbed garnet surrounded by Amp+Pl symplectite. The matrix consists mostly of Cpx+Pl symplectite, with local occurrence of atoll-Cpx around Qtz. (b) BSE image of Cpx-Pl symplectite in Be9918. In some places Cpx has broken down to amphibole. At the lower and right margin atoll-Cpx surrounds Qtz; in the top left section granoblastic Amp is surrounded by Pl.

A phase diagram computed for garnet-amphibolites from Monti della Motta in combination with calculated isopleths indicates that the garnet core composition equilibrated at conditions of ~675 °C and 2.1 GPa (Fig. 15a,b). The predicted stable mineral assemblage at these conditions is Grt + Cpx + Amp + Qtz + Rt (Fig. 15a). Isopleths for the rim composition do not intersect, which suggests that garnet was not only resorbed, but that the current rims were affected by diffusion. Apart from at the outer rim, Fe/(Fe+Mg) decreases consistently (Fig. 4f), which indicates that garnet grew in response to increasing temperature. The variation in grossular is very limited, and above 700 °C the calculated isopleths are closely aligned between 1.5 and 2.0 GPa, rendering assessment of the pressure evolution on the basis of garnet zoning impossible. However, modelling of garnet modal abundance indicates that decrease of pressure would be accompanied by garnet resorption. The inferred temperature increase was probably accompanied by constant or increasing pressure. During exhumation garnet was replaced by amphibole-plagioclase symplectite, likely by reaction with neighbouring pyroxene, whereas HP clinopyroxene, of which no relics survived, was replaced by symplectites of secondary clinopyroxene and plagioclase. Both textural information and the model suggest that the quartz phenocrysts surrounded by clinopyroxene-atolls are relics of the HP mineral assemblage, and that the clinopyroxene developed from HP pyroxene or from the pyroxene-quartz symplectites. The fact that rutile is replaced by ilmenite and the absence of titanite from these rocks, suggests once again that decompression was accompanied by heating. DOMINO modelling points at a decompressional overprint around 800–900 °C and 1.0–1.4 GPa, before final exhumation. Unfortunately, the model and the observed assemblage yield no additional confirmation of these high temperatures, and we consider these a tentative estimate. In this part of the Lepontine dome, conditions for

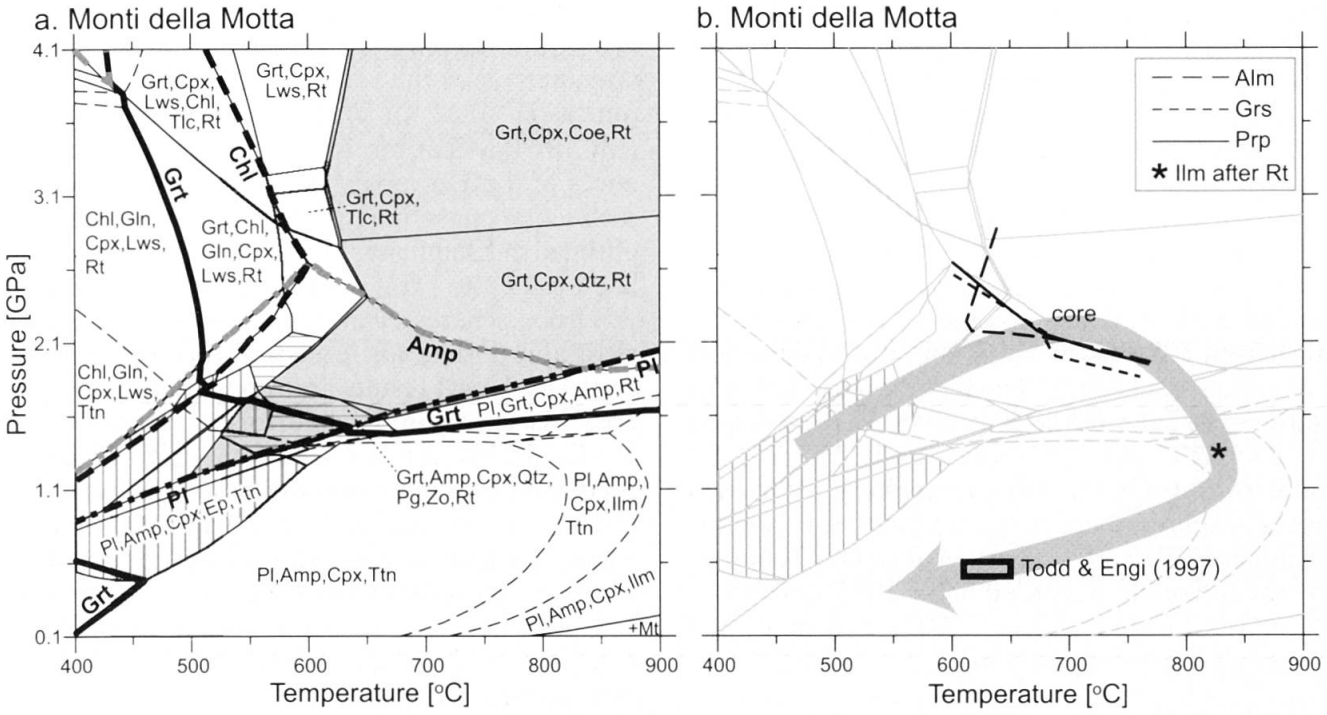

Fig. 15 (a) Computed phase relations for Monti della Motta sample Be9918 in the system CNFMASHTi, assuming fluid saturation and QFM-buffering. Grey shading indicates presence of quartz (very low modal abundance at eclogite conditions), horizontal stripes the presence of zoisite and vertical stripes denote epidote. Thick black line = garnet, black dash-dot line = plagioclase, grey dash-dot line = amphibole, thick black dashed line = chlorite, thin dashed lines = ilmenite-rutile-titanite. (b) Isopleths for garnet core composition calculated using DOMINO. Star marks the appearance of ilmenite after rutile and the black box indicate the PT conditions of the Barrovian overprint (Todd and Engi, 1997). Grey arrow indicates approximate PT-path for the sample.

the Barrovian regional metamorphism are ~630 ± 20 °C and 0.6 ± 0.05 GPa (Todd and Engi, 1997).

Gorduno

At Gorduno, mafic lenses from 10 cm to several tens of metres across are embedded in an orthogneiss-dominated basement, with some layers of metapelite and calcsilicate intercalated (e.g. Grubenmann, 1908; Möckel, 1969; Bocchio et al., 1985; Brouwer, 2000). Mafic rocks vary from plagioclase-amphibolite through garnet-amphibolite, to a few eclogites in the cores of larger lenses. Limited and localised availability of fluid, especially along the exhumation path, induced variations in the local effective bulk chemical composition leading to the development of textural domains with highly variable mineralogy (Tóth et al., 2000; Brouwer and Engi, 2005). The occurrence of such domains can be turned into an advantage by determining their chemical composition and using DOMINO to calculate appropriate phase diagrams for each of the domains. For samples from a single ~100 by 60 metre mafic lens this method

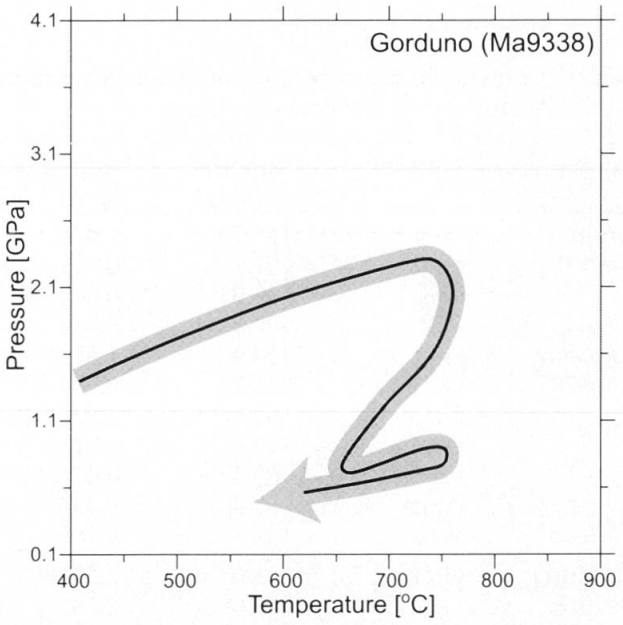

Fig. 16 PT-trajectory compiled using thermodynamic modelling of various chemical and textural domains in eclogites and garnet-amphibolites from the Gorduno body (Tóth et al., 2000; Brouwer and Engi, 2005). Modified after Brouwer and Engi (2005).

yielded a well-constrained PT-evolution (Fig. 16, compiled from Tóth et al. (2000) and Brouwer and Engi (2005)). Thermodynamic modelling led to the identification of a pseudomorph after lawsonite, which indicates that subduction occurred along a 'cool' trajectory. Garnet growth occurred between about 600 °C at 0.5 GPa and 700 °C at 2.0 GPa. Apart from the outer rim, garnet remnants (0.5–1 mm in diameter) are virtually homogeneous (Fig. 4g) and are thought to have grown in a restricted PT-window along that prograde trajectory (Tóth et al., 2000). The highest recorded pressures were 2.3 ± 0.3 GPa at 750 ± 50 °C, followed by cooling during decompression to 675 ± 25 °C and 0.8 ± 0.1 GPa. Due to regional Barrovian metamorphism these rocks recorded near-isobaric heating to 750 ± 40 °C (Tóth et al., 2000), followed by the regionally recorded 650 ± 20 °C and 0.55 ± 0.05 GPa (Todd and Engi, 1997), and then final cooling and decompression.

Lu–Hf geochronology of HP metamorphism

Samples from Alpe Arami, Alpe Repiano, Monti della Motta and Gorduno were dated by the Lu–Hf method (Table 3). Lu–Hf is a particularly attractive system for application to eclogites, because it can be used to date minerals from the HP mineral assemblage. Garnet has very high Lu–Hf ratios, resulting in a large separation of the parent and daughter isotopes (e.g. Duchêne et al., 1997). Chemical separation of Lu and Hf followed the procedure outlined by Kleinhanns et al. (2002), and analyses of the spiked solutions were carried out using the *Nu Instruments* multi-collector (MC) ICP-MS at the Institute of Geological Sciences of the University of Berne, Switzerland. Instrumental mass bias correction procedures are outlined in Kleinhanns et al (2002). Ages are calculated using the ^{176}Lu decay constant of $1.865 \cdot 10^{-11}$ yr^{-1} from Scherer et al. (2001), which is deemed most appropriate for terrestrial rocks (Söderlund et al., 2004). All results are reported with 2-sigma errors. Isochrons and their errors are calculated using Isoplot/Ex version 3.00 Beta (Ludwig, 2003). As the interpretation of some of our results is complicated, this is discussed extensively in a separate paper, to which we also refer for further details of analytical procedures (Brouwer et al., submitted). The interpretations of results for the two samples presented in that paper are briefly reported here, accompanied by the results for two additional samples and their geological significance.

The eclogite from Alpe Arami (Be9901) yielded a Lu–Hf multigrain isochron age of 36.6 ± 8.9 Ma (Fig. 17a, Brouwer,et al., submitted). This age is poorly constrained due to a relatively large error in the ^{176}Hf/^{177}Hf ratio of clinopyroxene and the small spread in ^{176}Lu/^{177}Hf. The age is within error of published ages, which were interpreted to date HP metamorphism (37.5 ± 2.2 Ma Grt–Cpx Sm–Nd age, Becker, 1993) and decompression melting after peak pressure (35.8 ± 2.2 Ma U–Pb

Table 3 Lu and Hf element and isotopic data for mineral separates and WR powders. In-run precision given as 2 standard errors in the last decimal places.

Sample	Mineral	Sample wt (mg)	Lu (ppm)	Hf (ppm)	^{176}Lu/^{177}Hf	^{176}Hf/^{177}Hf (± 2se abs)
Arami	Grt1	115.5	1.001	1.575	0.0899	0.283125 ±05
Be9901	Grt2	107.7	0.979	1.896	0.0731	0.283121 ±11
	Cpx	99.9	0.048	0.782	0.0086	0.283072 ±25
	WR	100.0	0.486	2.100	0.0327	0.283086 ±09
Repiano	Grt1	114.9	1.579	1.178	0.1897	0.283195 ±08
Rep9702	Grt2	115.2	0.989	0.591	0.2370	0.283167 ±13
	Grt3	85.4	1.221	0.714	0.2420	0.283237 ±12
	Grt4	113.2	0.911	1.033	0.1247	0.283126 ±07
	Cpx	85.4	0.076	0.974	0.0110	0.282967 ±11
	Amp	99.8	0.332	1.698	0.0276	0.282982 ±05
	WR	102.8	0.585	2.431	0.0340	0.283016 ±04
M. Motta	Grt1	115.0	2.554	1.222	0.2958	0.283225 ±07
Be9918	Grt2	112.6	2.185	1.485	0.2082	0.283312 ±06
	Amp	99.8	0.413	2.237	0.0261	0.283045 ±05
	WR	93.2	0.541	2.629	0.0291	0.283048 ±06
Gorduno	Grt-L	113.0	2.054	1.838	0.1581	0.283164 ±17
Ma9338	Grt-S	115.7	2.266	1.379	0.2325	0.283221 ±11
	Amp	95.1	0.229	1.732	0.0187	0.283069 ±05
	WR	100.1	0.560	2.790	0.0284	0.283083 ±06

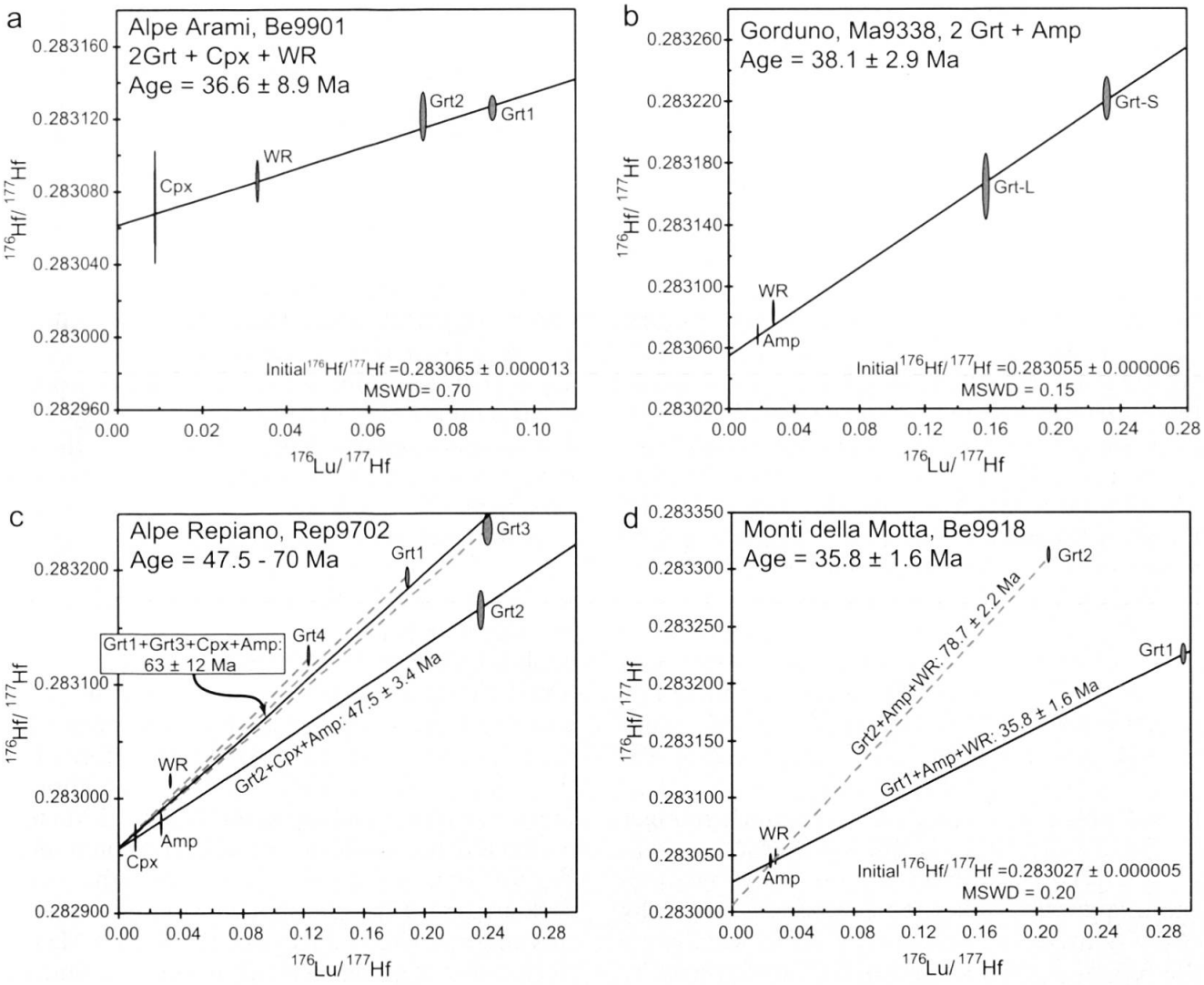

Fig. 17 Lu-Hf isochrons for four selected HP metamorphic rocks from the Central Swiss Alps. Abbreviations: Amp= amphibole, Cpx= omphacitic pyroxene, Grt= garnet, WR= whole rock powder. Data are in Table 3. (a) Alpe Arami, Be9901. (b) Gorduno, Ma9338. Grt-L separate grain size > 1 mm, Grt-S grain size 0.25-0.5 mm. (c) Alpe Repiano, Rep9702; MSWD and initial $^{176}Hf/^{177}Hf$ for various isochrons in Table 4. (d) Monti della Motta, Be9918. See text for discussion.

SHRIMP age of magmatic zircon rims, Gebauer, 1996). On the basis of the homogeneous distribution of major and trace elements in garnet (0.2–0.5 mm diameter) in this sample, the high temperatures this rock experienced during HP (~800 °C, ~2 GPa) and Barrovian metamorphism (700–750 °C, Brouwer, 2000) and considerations regarding diffusion of Lu and Hf in garnet, as well as recrystallisation, it is most likely that the Lu–Hf age reflects resetting not far below 800 °C (Brouwer, et al., submitted). Since Sm and Nd are also REE, and their diffusional behaviour is similar to that of Lu, it is likely that the previous Sm–Nd age (Becker, 1993) does not reflect crystallisation during HP metamorphism but cooling.

Garnet-amphibolite sample Ma9338 from Gorduno yields a three point isochron of 38.1 ± 2.9 Ma age (Fig. 17b). The whole-rock data plot slightly above the isochron, which may indicate the presence of some inherited component. However, despite careful petrography and electron microscopy no zircon at all has been observed in this sample. Since the four-point isochron results in the same age as the three-point isochron, the modal amount of inherited material must be very low. Garnet is thought to have grown in a small P-T interval, as indicated by the homogeneous composition of most of the garnet volume, whereas the marked change at the rim may reflect diffusion during the Barrovian overprint (Fig. 16). Since both large and small garnet yield the same age, it is most likely that the age reflects garnet growth around 38 Ma, affected only to a very minor extent by late diffusional resetting.

Lu–Hf geochronology on the partially retrogressed eclogite from Alpe Repiano (Rep9702)

yields a complicated pattern (Fig. 17c, Brouwer et al., submitted). Four analysed garnet separates of crystals and fragments in different size fractions have markedly different Lu–Hf compositions (Table 3). Garnet in the Repiano sample is coarse grained (ranging from 2 to 5 mm) and strongly zoned in major and trace elements. Using the Lu and Hf contents of the separates in combination with laser-ablation ICP-MS data of the Lu and Hf content of garnet, it is possible to identify one garnet separate (Grt4) with significantly lower Lu/Hf (Table 4, Brouwer et al., submitted). Zircon has very high Hf and much lower Lu contents, and the low Lu/Hf of this analysis suggests that the separate contained a zircon component, which leads us to exclude this separate from further consideration because zircon is known to disturb Hf systematics (Scherer et al., 2000). Because garnet major and trace element zoning survived the high metamorphic temperatures (Brouwer et al., submitted), we interpret the remaining analyses in terms of garnet growth, which may have been continuous, or in spurts. Separates dominated by garnet cores (Grt1 and Grt3) and the matrix minerals (Cpx, Amp) yield the oldest ages (up to 70.0 ± 2.9 Ma), whereas the separate dominated by garnet rims (Grt2) turns out to be much younger (47.5 ± 3.4 Ma, Table 4). The whole-rock analysis plots slightly above both of these isochrons, indicating a possible inherited component hosted by sparsely occurring zircon crystals. We can assess the role of a possible inherited Hf component by calculating an isochron with Grt1 and Grt3 and the whole-rock data, and comparison with the aforementioned Grt2–Grt3–Cpx–Amph isochron. The difference is on the order of 10 Ma, corresponding to 0.1% in the $^{176}Hf/^{177}Hf$. This estimate brackets the uncertainties related to the multigrain analysis and possible inherited Hf component. However, the change in Lu concentration of the separates, which is independent of the Hf problem, clearly shows that the ages obtained are related to the growth history of garnet. As shown in the phase diagram (Fig. 13), garnet grew along the prograde path between ~70 and 59 Ma (63 ± 12 Ma if garnet separates 1 and 3, clinopyroxene, amphibole and whole rock are used; Table 4; Brouwer, et al., submitted). Garnet rims equilibrated along the retrograde path (see section on petrology), which happened at 48 Ma or later.

As in the sample from Repiano, Lu–Hf geochronology of minerals from garnet amphibolite sample Be9918 from Monti della Motta is complicated (Fig. 17d, Tables 3,4). The compositions of the fractions dated produce two significantly different isochrons, which are controlled by the two garnet analyses. The two separates are two pickings from the same garnet concentrate with a 0.25–0.5 mm grain size. Garnet major element zoning (Fig. 4f) suggests that garnet may reflect a spread in crystallisation age (cf. Repiano), as well as effects of partial diffusional resetting, before cooling below its closure temperature (cf. Arami). Small zircon inclusions were observed in garnet cores, and the two garnet analyses show a marked difference in Lu/Hf (Table 4). It is therefore likely that Grt2 (with low Lu/Hf due to the additional Hf from zircon, resulting in the 78.7 ± 2.2 Ma age) is affected by a small, inherited zircon component. We note that no such effect is visible in the whole-rock analysis. This age is not considered further in this analysis. The younger age (35.8 ± 1.6 Ma) reflects a mix of garnet crystallisation sometime before ~36 Ma and a later diffusional resetting signature. This age thus represents an upper age limit for cooling after the Barrovian overprint.

The difficulties in deriving age constraints from Lu–Hf dating are related to (1) primary age zonation of the grains, which is usually not resolved in multigrain separates, (2) resetting by diffusion, and (3) inherited Hf signatures. The effect of primary age-zoned garnets shows up in the Repiano sample, which is best constrained using the

Table 4 Ages calculated using various separates for samples Rep9702 (Alpe Repiano) and Be9918 (Monti della Motta). Isochrons are calculated for different combinations of garnet separates with values for matrix phases and whole rock.

Sample	Separate	garnet grain-size (mm)	Lu (ppm)	Hf (ppm)	Lu/Hf	Age (Ma)	error	MSWD	Initial $^{176}Hf/^{177}Hf$
Alpe Repiano	G1/Px,Amp	> 1	1.6	1.2	1.33	70.0	2.9	1.5	0.282947
(Rep9702)	G2/Px,Amp	0.25–0.5	1.0	0.6	1.67	47.5	3.4	0.004	0.282957
	G3/Px,Amp	0.125–0.25	1.2	0.7	1.71	63.6	3.2	0.79	0.282950
	G4/Px,Amp	0.5–1	0.9	1.0	0.90	77	53	2.7	0.282946
	G1,G3/Px,Amp					63	12	5.7	0.282952
Monti della Motta	G1/Amp,WR	0.25-0.5	2.6	1.2	2.17	35.8	1.6	0.20	0.283027
(Be9918)	G2/Amp,WR	0.25-0.5	2.2	1.5	1.47	78.7	2.2	0.040	0.283006

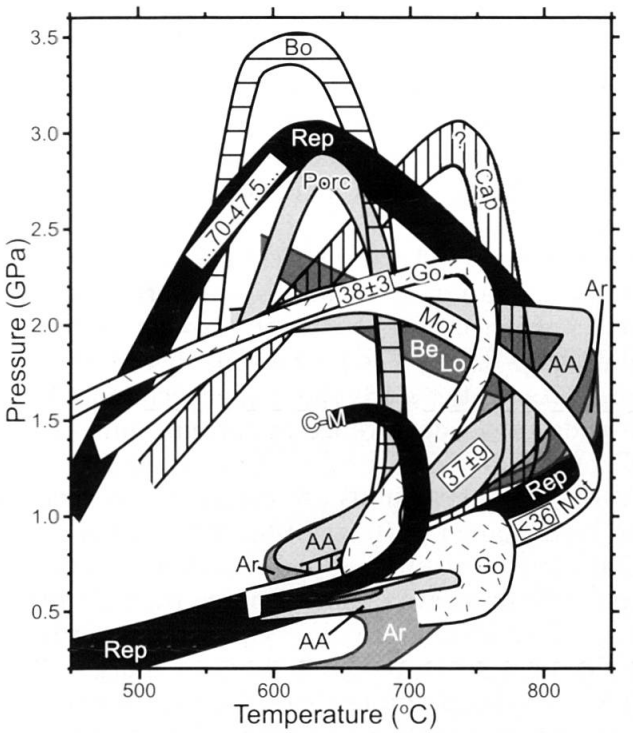

Fig. 18 Compilation of PT curves from the present study and the literature, obtained from fragments of the TAC units in the western part of the Southern Steep Belt. Abbreviations and references (numbers in brackets refer to locations numbers in Fig. 1 and Table 1): AA = [38] Alpe Arami (Fig. 10), Ar = Val d'Arbedo (Engi et al., 2001b), Be,Lo = Bellinzona, Locarno (Grandjean, 2001), Bo = [2] Bordoglio (Fig. 5b), C-M = Camughera-Moncucco (Keller et al., 2005), Cap = [5] Capoli (Fig. 9b), Go = [39] Gorduno (Fig. 16; Tóth et al., 2000; Brouwer and Engi, 2005), Mot = [36] Monti della Motta (Fig. 19b), Porc = [1] Porcaresc (Fig. 7b), Rep = [37] Alpe Repiano (Fig. 13b). Boxed numbers are Lu–Hf ages from this study, following the interpretations outlined in the text.

variation of Lu content of separates combined by LA-ICP-MS analysis (Brouwer, et al., submitted). In contrast, some process that enhanced diffusion or recrystallisation (partially) reset the Lu/Hf clock in the other samples (Arami, Gorduno, Monti della Motta). Inherited Hf is located in garnet or in accessory minerals, notably zircon. The probability that the samples dated in this study include pre-Alpine (Variscan) garnet relics is considered low for three reasons: (1) We have been unable to find any petrological evidence (e.g. resorbed cores) in any of the HP samples to suggest a polycyclic origin of garnet cores; (2) during the Alpine prograde evolution, rocks incorporated into the TAC were affected by penetrative polyphase deformation, which typically led to recrystallisation fabrics and obliterated much of the pre-Alpine imprint; (3) protolith ages determined for ophiolite relics (Stucki et al., 2003) are Jurassic, i.e. post-Variscan. Most zircon inclusions observed in garnet in the samples dated, are interpreted as exsolutions from the host phase. Inherited zircon crystals, however, appear to have affected one garnet separate in the sample from Monti della Motta and have also been documented in SHRIMP studies (Gebauer, 1996; Stucki et al., 2003). The effect of such zircons for the present samples has been assessed and the additional uncertainty due to inherited zircon on the isochron ages has been added to the ages obtained for the Repiano sample.

In summary, prograde garnet growth is at least indicated for the time range >70 to 59 Ma (Repiano). The petrological analysis presented above indicates that the early grown garnet most likely developed before the peak in pressure was reached. In the Central Alps (this study, Becker, 1993; Gebauer, 1996) the timing of peak pressures in the eclogites is still not clear, in part because of the high temperatures associated with these eclogites (compare Philippot et al., 2001). Important resetting (Arami) and/or growth (Gorduno) of garnet is constrained at ~38 Ma (in accordance with Sm/Nd ages by Becker (1993); and zircon SHRIMP ages by Gebauer (1996)).

Synthesis of metamorphic evolution and geodynamic framework

From the petrological and geochronological data presented in this paper emerges an overview of the metamorphic evolution of the southern part of the Lepontine Alps. Even when restricted to mafic bodies that preserve at least relics of HP metamorphism, a compilation of the PT-paths reconstructed for such bodies shows substantial variation in almost any respect (Fig. 18). Samples for which PT-conditions preceding HP metamorphism could be constrained show notable differences in the early P/T slope. In Gorduno, the identification of a pseudomorph after lawsonite indicates that the initial subduction trajectory was cool, whereas in Bordoglio the earliest temperature recorded is already quite high (~550 °C at 1.5–2.0 GPa). Additional striking differences are in the maximum pressures that were recorded by the different lenses (for example, from about 1.2 GPa in Vals (Löw, 1986; Löw, 1987; Dale and Holland, 2003) to ~3.4 GPa at Bordoglio), and the temperatures at which peak pressures were reached (between 600 and 750 °C). In the northern and central part of the Adula unit, a regionally coherent pressure gradient has been documented among the mafic lenses (Heinrich, 1986; Dale and Holland, 2003). In contrast, peak pressures in the

southern Adula and the SSB are variable (Fig. 18), but show no systematics amongst fragments, implying greater relative mobility. Garnet growth occurred before the samples reached their maximum recorded pressure and was dated at >70 Ma in the sample from Repiano. This age indicates that this fragment was subducted during early stages of Alpine convergence, when the Piemont-Ligurian ocean was subducted (compare HP ages in the Sesia unit: 65 Ma, Rubatto et al., 1999). In contrast, prograde garnet growth in the Gorduno sample was recorded much later, around 38 Ma. This allows a European margin provenance for the Gorduno lens, but does not exclude the possibility that it was derived from further south.

After HP metamorphism some lenses recorded heating during decompression (e.g. Repiano and Capoli, Fig. 18), some experienced initial cooling followed by reheating (e.g. Arbedo and Gorduno), whereas a third group lacks evidence of heating during decompression (e.g. Bordoglio). Temperatures reached during decompression vary between ~650 and 850 °C, and these temperatures were reached at markedly different pressures (between 2.0 and 0.5 GPa). The Lu–Hf data indicate that garnet recorded resetting at 37 ± 9 Ma in the Arami sample and sometime after 35.8 ± 1.6 Ma at Monti della Motta, providing an upper limit for the regional Barrovian overprint. During this overprint, producing migmatites and a suite of aplites and pegmatites, partial melting was widespread in the SSB (Burri et al., 2005), mostly dated between 28–25 Ma (Gebauer, 1996; Romer et al., 1996; Schärer et al., 1996). In the central Adula nappe staurolite growth resulted from a post nappe-stacking decompression reaction at 1.0–0.6 GPa and 600–650 °C, and was dated at 28.0 ± 2.3 Ma (Nagel, 2002). PT-trajectories for the various lenses converge in the window 0.4–0.8 GPa and 600–700 °C. This convergence is also reflected by the coherent patterns of isograds, isotherms, and isobars that reflect the Barrovian metamorphism in the Lepontine dome (Engi et al., 1995; Todd and Engi, 1997; Frey and Ferreiro Mählmann, 1999), which indicates that the tectonic stack had essentially acquired its present-day sequence when these isograds were recorded.

The highly variable PTt-evolution of mafic rocks in the Lepontine area (Fig. 18) constrains the tectonic scenario for the evolution along the plate boundary. HP metamorphism occurred due to subduction of the Piemont-Ligurian ocean, the Briançonnais continental fragment, the Valais oceanic realm and the southern margin of Europe beneath Apulia. Subduction was followed by continental collision, during which some of the previously subducted material was extruded to mid-crustal levels. Mafic und subordinate ultramafic lenses, most of them a few metres to about 100 m in size, which may now be within a few kilometres from one another and are surrounded by predominantly felsic country rocks, behaved as separate entities during subduction and subsequent exhumation to mid-crustal depths. In addition, the inferred protracted history of subduction, accretion, and exhumation of fragments with various speeds and residence times has now been confirmed by direct age dating. The new inventory of HP rocks presented in this study shows that such relics have a widespread occurrence in certain units of the Central Alps (Fig. 1): Adula, Cima Lunga, and the SSB. All of these units are therefore interpreted to be exhumed portions of the TAC (Engi et al., 2001a) and are thus mapped as mélange units. The mélange units are distinguishable by their lithological content, which differs from the underlying units derived from the European margin. The TAC is spatially more extensive than previously thought, especially west and northwest of Locarno, and its updated spatial relations appear on the new Tectonic and Petrographic Map of the Central Lepontine Alps (1:100'000, Berger and Mercolli, 2006).

Isolated garnet-amphibolite occurrences in the Simano nappe (Fig. 1) are not included in the TAC unit because they do not preserve relics of HP metamorphism. The maximum recorded pressure is ~1.2 GPa at 700 °C and was followed by cooling during decompression (Grandjean, 2001). Metasedimentary rocks of the Simano recorded intermediate pressures, in the range of 0.9–1.1 GPa (Rütti, 2003) for their earliest preserved phase of deformation and metamorphism. These P–T conditions likely pertain to the subduction of coherent nappes in the footwall of the TAC. After partial exhumation of the TAC, from pressures of ~0.6 GPa and less, the footwall units recorded the same metamorphic history as the TAC.

Conclusions

Eclogite relics in the western part of the Lepontine dome are widespread and more common than previously reported. The mafic lenses containing HP relics are enclosed in a basement composite of orthogneisses, paragneisses, schists, marble and calcsilicate rocks, along with some ultramafic fragments. The lenses are highly variable in size and recorded various PT-trajectories. New Lu–Hf geochronological data show that the fragments recorded eclogite-facies metamorphic conditions at different times, from >70 until ~38 Ma. These variations reflect the tectonic environment

in which these rocks developed. The HP fragments are all part of a lithosphere-scale tectonic mélange unit, which started its evolution as a TAC along the plate boundary, during convergence of Europe and Apulia. Within the TAC, lithospheric fragments were subducted, accreted and then exhumed, until the entire unit coalesced during the Lepontine Barrovian overprint. New Lu–Hf ages provide an upper age limit of ~36 Ma for Barrovian metamorphism. Samples to a variable degree retain a record of their individual PTt-trajectories depending on lithology, deformation and availability of fluids. The PTt-paths indicate that fragments moved at various speeds and had unequal residence times at various depths. The paleogeographic origin of tectonic fragments may sometimes be constrained by dating relics of HP metamorphism. However, because of the potentially different provenance of lenses, their variable residence times and their internal mobility, the TAC as a whole should not be thought of as a coherent crystalline nappe, representing a coherent basement unit upon which sedimentary rocks were deposited. Instead, the TAC may be considered a lithosphere-scale tectonic mélange, in which the zones („Züge") of the classical subdivision of the Southern Steep Belt represent tectonic slices of contrasting lithology, rather than a paleogeographic origin. The assembly of the TAC as a coherent Alpine tectonic unit is a late-Alpine feature and the details of its emplacement in the nappe stack remain to be fully worked out.

Acknowledgements

Financial support from Schweizerischer Nationalfonds (No. 20-63593.00 and 20020-101826) is gratefully acknowledged. We are grateful to Ilka Kleinhanns and Jan Kramers for their help with the geochronology. Thanks also to Paul Gräter, Ruedi Hänny, the Institute of Mineralogy and Petrography of the University of Basel, as well as the Basel Museum of Natural History who provided access to their sample collections. We gratefully acknowledge careful and constructive reviews by Stéphanie Duchêne, Jane Gilotti, Laurent Jolivet and Matthias Konrad-Schmolke that helped us improve this paper.

References

Ashworth, J.R., Sheplev, V.S., Khlestov, V.V. and Ananyev, V.A. (2004): An analysis of uncertainty in non-equilibrium and equilibrium geothermobarometry. *J. Metam. Geol.* **22**, 811–824.

Bächlin, R., Bianconi, F., Codoni, A., Dal Vesco, E., Knoblauch, P., Kündig, E., Reinhard, M., Spaenhauer, F., Spicher, A., Trommsdorff, V. and Wenk, E. (1974): Geologischer Atlas der Schweiz, sheet 1313, Bellinzona. Schweizerische Geologische Kommission, Bern.

Becker, H. (1993): Garnet peridotite and eclogite Sm–Nd mineral ages from the Lepontine dome (Swiss Alps): New evidence for Eocene high-pressure metamorphism in the central Alps. *Geology* **21**, 599–602.

Berger, A., Mercolli, I. and Engi, M. (2005): The central Lepontine Alps: Notes accompanying the tectonic and petrographic map sheet Sopra Ceneri (1:100' 000). *Schweiz. Mineral. Petrogr. Mitt.* **85**, 109–146.

Berger, A. and Mercolli, I. (2006): Tectonic and petrographic map of the central Lepontine Alps. 1:100' 000, carta geologica speciale N. 127. Federal Office of Topography, swisstopo, Wabern.

Berman, R.G. (1988): Internally-consistent thermodynamic data for minerals in the system Na_2O-K_2O-CaO-MgO-FeO-Fe_2O_3-Al_2O_3-SiO_2-TiO_2-H_2O-CO_2. *J. Petrol.* **29**, 445–522.

Berman, R.G. (1990): Mixing properties of Ca-Mg-Fe-Mn garnets. *Am. Mineral.* **75**, 328–344.

Berman, R.G. (1991): Thermobarometry using multi-equilibrium calculations: A new technique, with petrological applications. *Can. Mineral.* **29**, 833–855.

Bocchio, R., Liborio, G. and Mottana, A. (1985): Petrology of the amphibolitized eclogites of Gorduno, Lepontine Alps, Switzerland. *Chem. Geol.* **50**, 65–86.

Bocchio, R., De Capitani, L. and Ottolini, L. (2004): New chemical data on the clinopyroxene-garnet pair in the Alpe Arami eclogite, Central Alps, Switzerland. *Can. Mineral.* **42**, 1205–1219.

Brenker, F.E. and Brey, G.P. (1997): Reconstruction of the exhumation path of the Alpe Arami garnet-peridotite body from depths exceeding 160 km. *J. Metam. Geol.* **15**, 581–592.

Brouwer, F.M. (2000): Thermal evolution of high-pressure metamorphic rocks in the Alps. Published PhD thesis Utrecht University, Netherlands, *Geologica Ultraiectina* **199**, 221 pp.

Brouwer, F.M. and Engi, M. (2005): Staurolite and other aluminous phases in Alpine eclogites: Analysis of domain evolution. *Can. Mineral.* **43**, 105–128.

Brouwer, F.M., Berger, A., Engi, M., Mason, P.R.D. and Kleinhanns, I.C. (submitted): Lu–Hf geochronology of eclogites: What do we date? *Submitted to Chem. Geol.*,

Burri, T. (1999): Metamorphism and tectonics within the Vergeletto „Spoon" (Southern Vale Maggia, Ticino). Unpubl. MSc thesis, Universität Bern, 112 pp.

Burri, T. (2005): From high-pressure to migmatisation: on orogenic evolution of the Southern Lepontine (Central Alps of Switzerland / Italy). Unpubl. PhD thesis, Universität Bern, 150 pp.

Burri, T., Berger, A. and Engi, M. (2005): Tertiary migmatites in the Central Alps: Regional distribution, field relations, conditions of formation and tectonic implications. *Schweiz. Mineral. Petrogr. Mitt.* **85**, 215–232.

Carlson, W.D. (2002): Scales of disequilibrium and rates of equilibration during metamorphism. *Am. Mineral.* **87**, 185–204.

Chopin, C. (2003): Ultrahigh-pressure metamorphism: tracing continental crust into the mantle. *Earth Planet. Sci. Lett.* **212**, 1–14.

Cloos, M. and Shreve, R.L. (1988): Subduction-channel model of prism accretion, melange formation, sediment subduction, and subduction erosion at convergent plate margins: 2. Implications and discussion. *Pure Appl. Geoph.* **128**, 501–545.

Colombi, A. and Pfeifer, H.R. (1986): Ferrogabbroic and basaltic meta-eclogites from the Antrona mafic–ultramafic complex and the Centovalli-Locarno region (Italy and Southern Switzerland) – first results. *Schweiz. Mineral. Petrogr. Mitt.* **66**, 99–110.

Connolly, J.A.D. (1990): Multivariable phase diagrams: an algorithm based on generalized thermodynamics. *Am. J. Sci.* **290**, 666–718.

Connolly, J.A.D. and Petrini, K. (2002): An automated strategy for calculation of phase diagram sections and retrieval of rock properties as a function of physical conditions. *J. Metam. Geol.* **20**, 697–708.

Dale, J. and Holland, T.J.B. (2003): Geothermobarometry, P-T paths and metamorphic field gradients of high-pressure rocks from the Adula Nappe, Central Alps. *J. Metam. Geol.* **21**, 813–829.

Dale, J., Powell, R., White, R.W., Elmer, F.L. and Holland, T.J.B. (2005): A thermodynamic model for Ca-Na clinoamphiboles in Na_2O-CaO-FeO-MgO-Al_2O_3-SiO_2-H_2O-O for petrological calculations. *J. Metam. Geol.* **23**, 771–791.

de Capitani, C. and Brown, T.H. (1987): The computation of chemical equilibrium in complex systems containing non-ideal solutions. *Geochim. Cosmochim. Acta* **51**, 2639–2652.

de Capitani, C. (1994): Gleichgewichts-Phasendiagramme: Theorie und Software. *Eur. J. Mineral.* **6 Beiheft**, 48.

Degeling, H., Eggins, S. and Ellis, D.J. (2001): Zr budgets for metamorphic reactions, and the formation of zircon from garnet breakdown. *Mineral. Mag.* **65**, 749–758.

Dobrzhinetskaya, L., Green, H.W. and Wang, S. (1996): Alpe Arami: A peridotite massif from depths of more than 300 kilometers. *Science* **271**, 1841–1845.

Dobrzhinetskaya, L.F., Schweinehage, R., Massonne, H.J. and Green, H.W. (2002): Silica precipitates in omphacite from eclogite at Alpe Arami, Switzerland: evidence of deep subduction. *J. Metam. Geol.* **20**, 481–492.

Droop, G.T.R. (1987): A general equation for estimating Fe^{3+} concentrations in ferromagnesian silicates and oxides from microprobe analysis, using stoichiometric criteria. *Mineral. Mag.* **51**, 431–435.

Duchêne, S., Blichert-Toft, J., Luais, B., Télouk, P., Lardeaux, J.M. and Albarède, F. (1997): The Lu–Hf dating of garnets and the ages of the Alpine evolution high-pressure metamorphism. *Nature* **387**, 586–589.

Engi, M., Todd, C.S. and Schmatz, D.R. (1995): Tertiary metamorphic conditions in the eastern Lepontine Alps. *Schweiz. Mineral. Petrogr. Mitt.* **75**, 347–369.

Engi, M., Berger, A. and Roselle, G.T. (2001a): Role of the tectonic accretion channel in collisional orogeny. *Geology* **29**, 1143–1146.

Engi, M., Scherrer, N.C. and Burri, T. (2001b): Metamorphic evolution of pelitic rocks of the Monte Rosa nappe: Constraints from petrology and single grain monazite age data. *Schweiz. Mineral. Petrogr. Mitt.* **81**, 305–328.

Ernst, W.G. (1981): Petrogenesis of eclogites and peridotites from the Western and Ligurian Alps. *Am. Mineral.* **66**, 443–472.

Evans, T.P. (2004): A method for calculating effective bulk composition modification due to crystal fractionation in garnet-bearing schist: implications for isopleth thermobarometry. *J. Metam. Geol.* **22**, 547–557.

Federico, L., Crispini, L., Scambelluri, M. and Capponi, G. (2005): The different P-T histories recorded by HP blocks in a tectonic melange (ligurian Alps – NW Italy): Implications for subduction and exhumation processes. *Mitt. Österr. Miner. Ges.* **150**, 37.

Forster, M., Dunlap, J. and Lister, G.S. (2006): Tectonic shuffle zone in the Tso Morari region. *J. Asian Earth Sci.* **26**, 135.

Forster, R. (1947): Geologisch-petrographische Untersuchungen im Gebiete nördlich Locarno. *Schweiz. Mineral. Petrogr. Mitt.* **27**, 1–249.

Fraser, G., Ellis, D. and Eggins, S. (1997): Zirconium abundance in granulite-facies minerals, with implications for zircon geochronology in high-grade rocks. *Geology* **25**, 607–610.

Frey, M., Desmons, J. and Neubauer, F. (eds) (1999): The new metamorphic map of the Alps. *Schweiz. Mineral. Petrogr. Mitt.* **79**. 230 pp.

Frey, M. and Ferreiro Mählmann, R. (1999): Alpine evolution metamorphism in the Central Alps. *Schweiz. Mineral. Petrogr. Mitt.* **79**, 135–154.

Gebauer, D. (1996): A P-T-t path for an (ultra?-) high-pressure ultramafic/mafic rock-association and its felsic country-rocks based on SHRIMP-dating of magmatic and metamorphic zircon domains. Example: Alpe Arami (Central Swiss Alps). In: Basu, A. and Hart, S. (eds): *Earth processes: Reading the isotopic code, Geophysical Monograph.* **95**. American Geophysical Union, Washington, 307–330.

Gottschalk, M. (1997): Internally consistent thermodynamic data for rock forming minerals. *Eur. J. Mineral.* **9**, 175–223.

Grandjean, V. (2001): Petrographical evolution of mafic relics and their implication for the geodynamics of the Central Alps. Unpubl. PhD thesis, Universität Bern, 127 pp.

Gräter, P. and Wenk, E. (1998): Geologischer Atlas der Schweiz, sheet 1292, Maggia, draft version. Schweizerische Geologische Kommission, Bern.

Grubenmann, U. (1908): Granatolivinfels des Gordunotales und seine Begleitgesteine. *Viertelj. Naturf. Ges. Zürich* **53**, 129–156.

Gutzwiler, E. (1912): Injektionsgneise aus dem Kanton Tessin. Imprimeries Réunies, Lausanne, 64 pp.

Häuselmann, P. (1997): Zur Geologie des Val Vergeletto (Ti). Unpubl. MSc thesis, Universität Bern, 98 pp.

Heinrich, C.A. (1982): Kyanite-eclogite to amphibolite facies evolution of hydrous mafic and pelitic rocks, Adula nappe, Central Alps. *Contrib. Mineral. Petrol.* **81**, 30–38.

Heinrich, C.A. (1986): Eclogite facies regional metamorphism of hydrous mafic rocks in the Central Alpine Adula nappe. *J. Petrol.* **27**, 123–154.

Holland, T. and Blundy, J. (1994): Non-ideal interactions in calcic amphiboles and their bearing on amphibole-plagioclase thermometry. *Contrib. Mineral. Petrol.* **116**, 433–447.

Holland, T.J.B. and Powell, R. (1998): An internally-consistent thermodynamic data set for phases of petrological interest. *J. Metam. Geol.* **16**, 309–343.

Hoschek, G. (2004): Comparison of calculated P-T pseudosections for a kyanite eclogite from the Tauern Window, Eastern Alps, Austria. *Eur. J. Mineral.* **16**, 59–72.

Keller, L.M., Abart, R., Schmid, S.M. and de Capitani, C. (2005): Phase relations and chemical composition of phengite and paragonite in pelitic schists during decompression: a case study from the Monte Rosa nappe and Camughera-Moncucco Unit, Western Alps. *J. Petrol.* **46**, 2145–2166.

Kleinhanns, I.C., Kreissig, K., Kamber, B.S., Meisel, T., Nägler, T.F. and Kramers, J.D. (2002): Combined chemical separation of Lu, Hf, Sm, Nd, and REE's from a single rock digest: Precise and accurate isotope determinations of Lu–Hf and Sm–Nd using multicollector-ICPMS. *Anal. Chem.* **74**, 67–73.

Kobe, H. (1956): Geologisch-Petrografische Untersuchungen in der Tessiner Wurzelzone zwischen Vergeletto-Onsernone und Valle Maggia. *Schweiz. Mineral. Petrogr. Mitt.* **36**, 244–348.

Konrad-Schmolke, M., Handy, M.R., Babist, J. and O'Brien, P.J. (2005): Thermodynamic modelling of diffusion-controlled garnet growth. *Contrib. Mineral. Petrol.* **149**, 181–195.

Köppel, V., Günthert, A. and Grünenfelder, M. (1981): Patterns of U–Pb zircon and monazite ages in polymetamorphic rocks in the Swiss Alps. *Schweiz. Mineral. Petrogr. Mitt.* **61**, 97–119.

Kretz, R. (1983): Symbols for rock-forming minerals. *Am. Mineral.* **68**, 277–279.

Liu, X., Wei, C., Li, S., Dong, S. and Liu, J. (2004): Thermobaric structure of a traverse across western Dabieshan: implications for collision tectonics between the Sino-Korean and Yangtze cratons. *J. Metam. Geol.* **22**, 361–379.

Löw, S. (1986): Ein tektono-metamorphes Entwicklungsmodell der nördlichen Adula-Decke. *Schweiz. Mineral. Petrogr. Mitt.* **66**, 129–134.

Löw, S. (1987): Die tektono-metamorphe Entwicklung der Nördlichen Adula-Decke. *Beiträge zur Geologischen Karte der Schweiz* **161** (Neue Folge). Stämpfli & Cie., Bern, 84 pp.

Ludwig, K.R. (2003): User's manual for Isoplot 3.00. A geochronological toolkit for Microsoft Excel. *Berkeley Geochronology Center Special Publication* **4**. 71 pp.

Mancktelow, N.S. (1991): Neogene lateral extension during convergence in the Central Alps: Evidence from interrelated faulting and backfolding around the Simplonpass (Switzerland). *Tectonophysics* **215**, 295–317.

Meyre, C., de Capitani, C. and Partzsch, J.H. (1997): A ternary solid solution model for omphacite and its application to geothermobarometry of eclogites from the Middle Adula nappe (Central Alps, Switzerland). *J. Metam. Geol.* **15**, 687–700.

Möckel, J.R. (1969): Structural petrology of the garnet-peridotite of Alpe Arami (Ticino, Switzerland). *Leidse Geol. Meded.* **42**, 61–130.

Nagel, T. (2002): Metamorphic and structural history of the southern Adula nappe (Graubünden, Switzerland). Unpubl. PhD thesis, Universität Basel, 103 pp.

Nakamura, D. (2002): Kinetics of decompressional reactions in eclogitic rocks – formation of plagioclase coronas around kyanite. *J. Metam. Geol.* **20**, 325–333.

Nimis, P. and Trommsdorff, V. (2001): Revised thermobarometry of Alpe Arami and other garnet peridotites from the central Alps. *J. Petrol.* **42**, 103–115.

Olker, B., Altherr, R. and Paquin, J. (2003): Fast exhumation of the ultrahigh-pressure Alpe Arami garnet peridotite (Central Alps, Switzerland): constraints from geospeedometry and thermal modelling. *J. Metam. Geol.* **21**, 395–402.

Paquin, J. and Altherr, R. (2001): New constraints on the P-T evolution of the Alpe Arami garnet peridotite body (Central Alps, Switzerland). *J. Petrol.* **42**, 1119–1140.

Pfeifer, H.R., Colombi, A., Ganguin, J., Hunziker, J.C., Oberhänsli, R. and Santini, L. (1991): Relics of high-pressure metamorphism in different lithologies of the Central Alps, an updated inventory. *Schweiz. Mineral. Petrogr. Mitt.* **71**, 441–451.

Pfiffner, M. and Trommsdorff, V. (1998): The high-pressure ultramafic-mafic-carbonate suite of Cima Lunga-Adula, Central Alps: Excursions to Cima di Gagnone and Alpe Arami. *Schweiz. Mineral. Petrogr. Mitt.* **78**, 337–354.

Philippot, P., Blichert-Toft, J., Perchuk, A., Costa, S. and Gerasimov, V. (2001): Lu–Hf and Ar–Ar chronometry supports extreme rate of subduction zone metamorphism deduced from geospeedometry. *Tectonophysics* **342**, 23–38.

Powell, R., Holland, T. and Worley, B. (1998): Calculating phase diagrams involving solid solutions via non-linear equations, with examples using THERMOCALC. *J. Metam. Geol.* **16**, 577–588.

Romer, R.L., Schärer, U. and Steck, A. (1996): Alpine and pre-Alpine magmatism in the root-zone of the western Central Alps. *Contrib. Mineral. Petrol.* **123**, 138–158.

Rubatto, D., Gebauer, D. and Compagnoni, R. (1999): Dating of eclogite-facies zircons: the age of Alpine evolution metamorphism in the Sesia-Lanzo Zone (Western Alps). *Earth Planet. Sci. Lett.* **167**, 141–158.

Rütti, R. (2003): The tectono-metamorphic evolution of the northwestern Simano Nappe (Central Alps, Switzerland). Unpubl. PhD thesis no. 15149, ETH Zürich, 111 pp.

Schärer, U., Cosca, M., Steck, A. and Hunziker, J. (1996): Termination of major ductile strike-slip shear and differential cooling along the Insubric Line (Central Alps); U–Pb, Rb–Sr and $^{40}Ar/^{39}Ar$ ages of cross-cutting pegmatites. *Earth Planet. Sci. Lett.* **142**, 331351.

Scherer, E., Münker, C. and Mezger, K. (2001): Calibration of the lutetium-hafnium clock. *Science* **293**, 683–687.

Scherer, E.E., Cameron, K.L. and Blichert-Toft, J. (2000): Lu–Hf garnet geochronology: Closure temperature relative to the Sm–Nd system and the effects of trace mineral inclusions. *Geochim. Cosmochim. Acta* **64**, 3413–3432.

Schlunegger, F. and Simpson, G. (2002): Possible erosional control on lateral growth of the European Central Alps. *Geology* **30**, 907–910.

Schmid, S.M., Aebli, H.R., Heller, F. and Zingg, A. (1989): The role of the Periadriatic Line in the tectonic evolution of the Alps. In: Coward, M.P., Dietrich, D. and Park, R.G. (eds): Alpine Tectonics. *Spec. Publ. Geol. Soc. London* **45**. 153–171.

Schmid, S.M., Pfiffner, O.A., Froitzheim, N., Schönborn, G. and Kissling, E. (1996): Geophysical-geological transect and tectonic evolution of the Swiss-Italian Alps. *Tectonics* **15**, 1036–1064.

Schmid, S.M., Fügenschuh, B., Kissling, E. and Schuster, R. (2004): Tectonic map and overall architecture of the Alpine orogen. *Eclog. geol. Helv.* **97**, 93–117.

Söderlund, U., Patchett, P.J., Vervoort, J.D. and Isachsen, C.E. (2004): The ^{176}Lu decay constant determined by Lu–Hf and U–Pb isotope systematics of precambrian mafic intrusions. *Earth Planet. Sci. Lett.* **219**, 311–324.

Spicher, A. (1980): Tektonische Karte der Schweiz. 2nd ed. Schweizerische Geologische Kommission, Bern.

Stöckhert, B. and Gerya, T.V. (2005): Pre-collisional high pressure metamorphism and nappe tectonics at active continental margins: a numerical simulation. *Terra Nova* **17**, 102–110.

Stucki, A., Rubatto, D. and Trommsdorff, V. (2003): Mesozoic ophiolite relics in the Southern Steep Belt of the Central Alps. *Schweiz. Mineral. Petrogr. Mitt.* **83**, 285–299.

Terry, M.P., Robinson, P. and Krogh Ravna, E.J. (2000): Kyanite eclogite thermobarometry and evidence for thrusting of UHP over HP metamorphic rocks, Nordøyane, Western Gneiss Region, Norway. *Am. Mineral.* **85**, 1637–1650.

Timar-Geng, Z., Grujic, D. and Rahn, M. (2004): Deformation at the Leventina-Simano nappe boundary, Central Alps, Switzerland. *Eclog. geol. Helv.* **97**, 265–278.

Todd, C.S. and Engi, M. (1997): Metamorphic field gradients in the Central Alps. *J. Metam. Geol.* **15**, 513–530.

Tomkins, H.S., Williams, I.S. and Ellis, D.J. (2005): In situ U–Pb dating of zircon formed from retrograde garnet breakdown during decompression in Rogaland, SW Norway. *J. Metam. Geol.* **23**, 201–215.

Tóth, T.M., Grandjean, V. and Engi, M. (2000): Polyphase evolution and reaction sequence of compositional domains in metabasalt: a model based on local chemical equilibrium and metamorphic differentiation. *Geol. J.* **35**, 163–183.

Trommsdorff, V. (1990): Metamorphism and tectonics in the central Alps: the Alpine evolution lithospheric mélange of Cima Lunga and Adula. *Mem. Soc. Geol. It.* **45**, 39–49.

Trommsdorff, V., Hermann, J., Müntener, O., Pfiffner, M. and Risold, A.C. (2000): Geodynamic cycles of subcontinental lithosphere in the Central Alps and the Arami enigma. *J. Geodyn.* **30**, 77–92.

van Westrenen, W., Blundy, J.D. and Wood, B.J. (2001): High field strength element/rare earth element fractionation during partial melting in the presence of garnet: Implications for identification of mantle heterogeneities. *Geochem. Geophys. Geosyst.* **2**, 19, DOI 10.1029/2000GC000133.

Wang, H.S. (1939): Petrographische Untersuchungen im Gebiet der Zone von Bellinzona. *Schweiz. Mineral. Petrogr. Mitt.* **19**, 21–199.

Wenk, E. (1953): Prinzipielles zur geologisch-tektonischen Gliederung des Penninikums im zentralen Tessin. *Eclog. geol. Helv.* **46**, 9–21.

Woodland, A.B., Seitz, H.M., Altherr, R., Marschall, H., Olker, B. and Ludwig, T. (2002): Li abundances in eclogite minerals: a clue to a crustal or mantle origin? *Contrib. Mineral. Petrol.* **143**, 587–601.

Received 29August 2005
Accepted 13 April 2006
Editorial handling: R. Gieré